

RESEARCH ARTICLES

Dothideomycete–Plant Interactions Illuminated by Genome Sequencing and EST Analysis of the Wheat Pathogen *Stagonospora nodorum*

James K. Hane,^{a,1} Rohan G.T. Lowe,^{a,1} Peter S. Solomon,^a Kar-Chun Tan,^a Conrad L. Schoch,^b Joseph W. Spatafora,^b Pedro W. Crous,^c Chinappa Kodira,^d Bruce W. Birren,^d James E. Galagan,^d Stefano F.F. Torriani,^e Bruce A. McDonald,^e and Richard P. Oliver^{a,2}

^a Australian Centre for Necrotrophic Fungal Pathogens, Murdoch University, WA 6150, Australia

^b Department of Botany and Plant Pathology, Oregon State University, Corvallis, Oregon 97331

^c Centraalbureau voor Schimmelcultures, 3508 AD Utrecht, The Netherlands

^d The Broad Institute, Cambridge, Massachusetts 02141-2023

^e Plant Pathology, Institute of Integrative Biology, LFW B16 8092 Zurich, Switzerland

Stagonospora nodorum is a major necrotrophic fungal pathogen of wheat (*Triticum aestivum*) and a member of the Dothideomycetes, a large fungal taxon that includes many important plant pathogens affecting all major crop plant families. Here, we report the acquisition and initial analysis of a draft genome sequence for this fungus. The assembly comprises 37,164,227 bp of nuclear DNA contained in 107 scaffolds. The circular mitochondrial genome comprises 49,761 bp encoding 46 genes, including four that are intron encoded. The nuclear genome assembly contains 26 classes of repetitive DNA, comprising 4.5% of the genome. Some of the repeats show evidence of repeat-induced point mutations consistent with a frequent sexual cycle. ESTs and gene prediction models support a minimum of 10,762 nuclear genes. Extensive orthology was found between the polyketide synthase family in *S. nodorum* and *Cochliobolus heterostrophus*, suggesting an ancient origin and conserved functions for these genes. A striking feature of the gene catalog was the large number of genes predicted to encode secreted proteins; the majority has no meaningful similarity to any other known genes. It is likely that genes for host-specific toxins, in addition to ToxA, will be found among this group. ESTs obtained from axenic mycelium grown on oleate (chosen to mimic early infection) and late-stage lesions sporulating on wheat leaves were obtained. Statistical analysis shows that transcripts encoding proteins involved in protein synthesis and in the production of extracellular proteases, cellulases, and xylanases predominate in the infection library. This suggests that the fungus is dependant on the degradation of wheat macromolecular constituents to provide the carbon skeletons and energy for the synthesis of proteins and other components destined for the developing pycnidiospores.

INTRODUCTION

Stagonospora nodorum (syn. *Phaeosphaeria*) is a major pathogen of wheat (*Triticum aestivum*) in most wheat-growing areas of the world. It is the major cause of losses due to foliar pathogens in Western Australia and north central and northeastern North America (Solomon et al., 2006a), and until the 1970s, it was the major foliar necrotrophic pathogen in Europe (Bearchell et al., 2005). Infection begins when spores (ascospores or asexual pycnidiospores) land on leaf tissue (Bathgate and Loughman, 2001; Solomon et al., 2006b). The spores rapidly germinate to produce hyphae that invade the leaf, using hyphopodia to gain

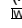
entry to epidermal cells or by growing directly through stomata (Solomon et al., 2006b). The hyphae rapidly colonize the leaves and begin to produce pycnidia in 7 to 10 d. The infection has been divided into three metabolic phases (Solomon et al., 2003a). The first phase is penetration of the host epidermis and is fuelled predominantly by lipid stores in the spores (Solomon et al., 2004a); the second is proliferation throughout the interior of the leaf, involves toxin release (Liu et al., 2006), and uses host-derived simple carbohydrate sources (Solomon et al., 2004a); the final phase produces the new spores, but so far the metabolic requirements for pycnidiation are unclear.

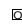
The infection epidemiology follows a polycyclic pattern with repeated cycles of both asexual (Bathgate and Loughman, 2001) and sexual (B.A. McDonald, unpublished data) infection throughout the growing season. New rounds of infection are initiated by rain-splash of pycnidiospores and wind dispersal of ascospores. Eventually, wheat heads become infected, causing the glume blotch symptom. In Mediterranean climates, the fungus overwinters in senescent straw and stubble. Seed transmission can be important but is readily controlled by fungicides. Infected stubble harbors the pseudothecia that produce airborne (Bathgate

¹ These authors contributed equally to this work.

² Address correspondence to roliver@murdoch.edu.au.

The author responsible for distribution of materials integral to the findings presented in this article in accordance with the policy described in the Instructions for Authors (www.plantcell.org) is: Richard P. Oliver (roliver@murdoch.edu.au).

 Online version contains Web-only data.

 Open Access articles can be viewed online without a subscription. www.plantcell.org/cgi/doi/10.1105/tpc.107.052829

and Loughman, 2001), heterothallic (Bennett et al., 2003) ascospores to reinitiate the infection in the following growing season. Epidemiological and population genetic evidence suggest that the fungus undergoes meiosis in the field regularly and that gene flow is global (Stukenbrock et al., 2006).

S. nodorum is a member of the Dothideomycetes class of filamentous fungi. This is a newly recognized major class that broadly replaced the long-recognized loculoascomycetes (Winka and Eriksson, 1997) and includes the causal organisms of many economically important plant diseases; notable examples are black leg (*Leptosphaeria maculans*), southern maize (*Zea mays*) leaf blight (*Cochliobolus heterostrophus*), barley (*Hordeum vulgare*) net blotch (*Pyrenophora teres*), apple scab (*Venturia inaequalis*), black sigatoka (*Mycosphaerella fijiensis*) of banana (*Musa* spp), wheat leaf blotch (*M. graminicola*), tomato (*Solanum lycopersicum*) leaf mold (*Passalora fulva*), and Ascochyta blight of many legume species (*Ascochyta* spp). The taxon also includes large numbers of saprobic species occurring on substrates ranging from dung to plant debris, a few species associated with animals, and several lichenized species (Del Prado et al., 2006).

Many plant pathogens in this group produce host-specific toxins (Wolpert et al., 2002). These molecules interact with specific host factors to produce disease symptoms only in selected genotypes of specific plant hosts. Well-known examples are found in *Alternaria alternata*, *Cochliobolus heterostrophus*, and *Pyrenophora tritici-repentis*, while species in the genera *Mycosphaerella*, *Corynespora*, and *Stemphylium* are also thought to produce host-specific toxins (Agrios, 2005). Proteinaceous host-specific toxins have recently been shown to be important virulence determinants in *S. nodorum* (Liu et al., 2004a, 2004b), including one whose gene is thought to have been interspecifically transferred to the wheat tan spot pathogen, *P. tritici-repentis* (Friesen et al., 2006). Only one example of a host-specific toxin has been identified outside of the Dothideomycetes (Wolpert et al., 2002). Non-host-specific toxins produced by species in this group include cercosporin (*Cercospora*) and solanopyrone (*Ascochyta*) but are also produced by many other fungal taxa (Agrios, 2005).

S. nodorum is an experimentally tractable organism, which is easily handled in defined media, was one of the first fungal pathogens to be genetically manipulated (Cooley et al., 1988), and has been a model for fungicide development (Dancer et al., 1999). Molecular analysis of pathogenicity determinants is aided by facile tools for gene ablation and rapid in vitro phenotypic screens, and thus far, a small number of genes required for pathogenicity have been identified (Cooley et al., 1988; Bailey et al., 1996; Bindschedler et al., 2003; Solomon et al., 2003b, 2004a, 2004b, 2005, 2006a). It has thus emerged as a model for dothideomycete pathology.

Whole-genome sequences have been described for a handful of fungal saprobes and pathogens (Galagan et al., 2003, 2005; Jones et al., 2004; Dean et al., 2005; Kamper et al., 2006). Here, we present an initial analysis of the genome sequence of the dothideomycete *S. nodorum*. Gene expression studies using EST libraries from axenic mycelium and heavily infected wheat leaves complement the genome sequence and provide a broad-based analysis of the genomic basis of infection by *S. nodorum*.

RESULTS

Acquisition and Analysis of the Genome Sequence

The genome sequence was obtained using a whole-genome shotgun approach. Approximately 10× sequence coverage was obtained as paired-end reads from plasmids of 4 and 10 kb plus 40-kb fosmids. Reads were assembled using Arachne (Jaffe et al., 2003), forming 496 contigs totaling 37,071 kb. The contig N50 was 179 kb, meaning an average base in the assembly lies within a contig of at least 179 kb. Greater than 98% of the bases in the assembly have a consensus quality score of ≥ 40 , corresponding to the standard error rate of fully finished sequence. The contigs are connected in 109 scaffolds spanning 37,202 kb with a scaffold N50 of 1.05 Mb. More than 50% of the genome is contained in the 13 largest scaffolds. Within the scaffolds, only ~ 140 kb is estimated to lie within sequence gaps. Thus, in terms of representation, contiguity, and sequence accuracy, the draft assembly is of high quality. The mitochondrial genome comprises a circle of 49,761 bp (GenBank accession number EU053989). It replaces two of the auto-assembled scaffolds, 52 and 65. The nuclear genome is therefore assembled in 107 scaffolds of total length 37,164,227 bp.

General features of the assembly are described in Table 1. As detailed below, the genomic sequencing was complemented by sequencing EST libraries. One library was constructed from axenically grown mycelium, and after removing vector, poly(A) sequences, poor-quality sequences, and sequences < 100 bp, there were 7750 remaining ESTs. Of these, 97.6% mapped to the genome assembly via Sim4, and 1.4% mapped to unassembled reads. This indicates that the assembly has achieved good coverage of the genome. In all, seven EST contigs and 13 singletons clustered to the unassembled reads.

Analysis of Repetitive Elements

Repetitive elements were identified de novo by identifying sequence elements that existed in 10 or more copies, were greater than 200 bp, and exhibited $> 65\%$ sequence identity. The analysis revealed the presence of 25 repeat classes. Table 2 lists the general features of the repeats (see Supplemental Data Set 1 online). Only three, Molly, Pixie, and Elsa, had been detected earlier (GenBank accession numbers AJ277502, AJ277503, and AJ277966, respectively). Molly, Pixie, X15, and R37 show

Table 1. The Assembly of the *S. nodorum* Nuclear Genome Sequence

Scaffold count	107
Total/bp	37,164,227
Coverage	$\sim 10\times$
G + C %	50.3%
Scaffold minimum length/bp	2,005
Scaffold maximum length/bp	2,531,949
Scaffold median length/bp	32,376
Scaffold mean length/bp	347,329
Gaps/number	387
Total length of gaps/bp	146,025
Max length of gap/bp	11,204
Median length of gap/bp	325

Table 2. Features of Repetitive Element Classes Found in the Nuclear Genome

Repeat Name	Class	Count	Full Length (bp)	Occupied (bp)	Percentage of Genome	RIP ^a
Subtelomeric						
R22	Telomeric repeat	23	678	12,565	0.03	No
X15	Telomeric repeat/transposon or remnant	37	6,231	89,126	0.24	No
X26	Telomeric repeat	38	4,628	77,020	0.21	No
X35	Telomeric repeat	19	1,157	14,393	0.04	No
X48	Telomeric repeat	22	265	5,631	0.02	No
Ribosomal						
Y1	rDNA repeat	113	9,358	40,1890	1.08	No
Other						
Elsa	Transposon	17	5,240	34,287	0.09	Yes
Molly	Transposon	40	1,862	50,453	0.14	Yes
Pixie	Transposon	28	1,845	39,148	0.11	No
R10	Unknown	59	1,241	44,018	0.12	No
R25	Unknown	23	3,320	44,860	0.12	No
R31	Unknown	23	3,031	40,267	0.11	No
R37	Transposon or remnant	98	1,603	104,915	0.28	No
R38	Unknown	25	358	8,556	0.02	No
R39	Unknown	29	2,050	35,758	0.10	No
R51	Unknown	39	833	25,538	0.07	No
R8	Unknown	48	9,143	275,643	0.74	No
R9	Transposon or remnant	72	4,108	163,739	0.44	No
X0	Unknown	76	3,862	145,268	0.39	No
X11	Transposon or remnant	36	8,555	128,638	0.35	No
X12	Unknown	29	2,263	25,369	0.07	No
X23	Unknown	29	685	11,679	0.03	No
X28	Unknown	30	1,784	32,002	0.09	No
X3	Unknown	213	9,364	463,438	1.24	No
X36	Unknown	10	512	5,067	0.01	No
X96	Unknown	14	308	4,321	0.01	No
Sum					4.52	

^aEvidence from the alignment that the repeat has been subjected to RIP mutation.

sequence characteristics of inverted terminal repeat-containing transposons, while Elsa, R9, and X11 appear to be retrotransposons. Repetitive elements were found individually throughout the genome but were often found in clusters spanning several kilobases.

Telomere-associated repeats were identified by searching for examples of the canonical telomere repeat TTAGGG at the termini of auto-assembled scaffolds. Physically linked repetitive sequences were then analyzed for association with the TTAGGG sequence repeats. Between 19 and 38 copies of telomere-associated repeats were found in the assembly.

Repeat-induced point (RIP) mutation is a fungal-specific genome-cleansing process that detects repeated DNA at meiosis and introduces C-to-T mutations into the copies (Cambareri et al., 1989). Using the parameters defined for *Magnaporthe grisea* (Dean et al., 2005), we identified RIP-like characteristics in several of the repeat classes (Table 2; see Supplemental Data Set 1 online). The transposons Molly and Elsa were the most clearly affected classes. None of the telomere-associated repeats displayed RIP characteristics.

Mitochondrial Genome

The mitochondrial genome of *S. nodorum* assembled as a circular molecule of 49,761 bp, with an overall G + C content

of 29.4%. It contains the typical genes encoding 12 inner mitochondrial membrane proteins involved in electron transport and coupled oxidative phosphorylation (*nad1-6* and *nad4L*, *cytb*, *cox1-3*, and *atp6*), the 5S ribosomal protein, three open reading frames (ORFs) of unknown function, and genes for the large and small rRNAs (*rnl* and *rns*) (Figure 1). The genes were coded on both DNA strands. The 27 tRNAs can carry all 20 amino acids. All tRNA secondary structures showed the expected cloverleaf form, but tRNA-Thr and tRNA-Phe had nine nucleotides in the anticodon loop instead of the typical seven, and tRNA-Arg2 had 11 nucleotides in its anticodon loop (Lowe and Eddy, 1997).

Gene Content

The initial gene prediction process identified 16,957 gene models of which 16,586 were located on the 107 nuclear scaffolds. A revised gene prediction procedure, using new ESTs (see below) and 795 fully supported and manually annotated gene models, identified 10,762 version 2 nuclear gene models. Of these, 617 genes corresponded to a merging of version 1 genes; in 50 cases, three prior gene models were merged, and in one case, four genes were merged. ESTs that aligned to unassembled reads identified one supported gene (SNOG_20000.2). A total of 5354 version 1 gene models were not supported but did not

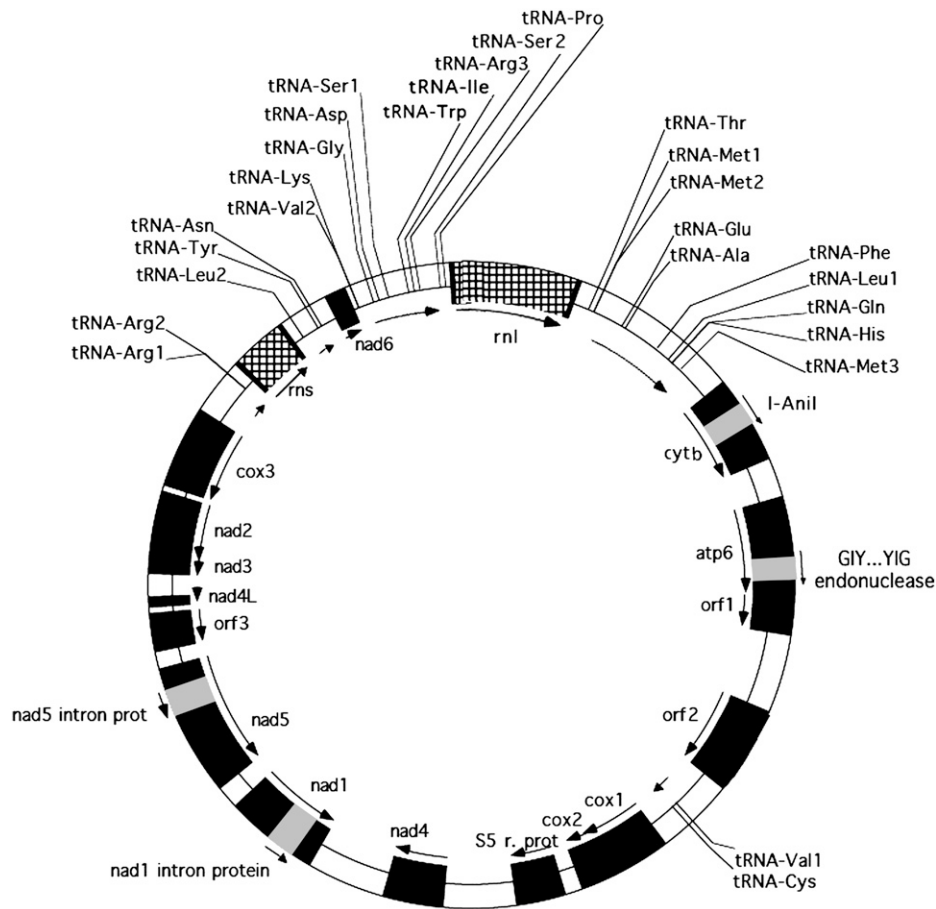


Figure 1. The Structure of the Mitochondrial Genome.

Black segments are exons, hatched segments are rRNA genes, and white segments are introns. The direction of transcription is indicated with the arrows.

conflict with second-round predictions. We therefore conclude that *S. nodorum* contains a minimum of 10,762 nuclear genes of which all but 125 are supported by two gene prediction procedures and 2696 are supported by direct experimental evidence via EST alignment. These genes, with an identification format SNOG_xxxxx.2, were compared with the GenBank nonredundant protein database at the National Center for Biotechnology Information (NCBI). Informative (not hypothetical, predicted, putative, or unknown) BLASTP (Altschul et al., 1990) hits with e -values $<1 \times 10^{-6}$ were found for 7116 genes (see Supplemental Data Set 2 online). It is estimated that at least 46.6% of the nuclear genome is transcribed and 38.8% is translated.

The 5354 gene models without support from the reannotation have unaltered accession numbers as SNOG_xxxxx.1 and are retained for further possible validation and analysis. As 952 of these unsupported gene models have BLASTP hits with e -values $<1 \times 10^{-6}$, we predict that some will be validated as new evidence emerges.

Gene Expression during Infection

Two EST libraries were constructed and analyzed as part of this project. An in vitro library was constructed from axenic fungal

mycelium transferred to media with oleate as the sole carbon source; this is referred to as the oleate library. An in planta library was made from bulked sporulating disease lesions on wheat 9, 10, and 11 d after infection (DAI). For both libraries, 5000 random clones were sequenced in both directions. The oleate library was entirely fungal and hence particularly suited for primary genome annotation purposes. The lipid growth media was chosen to replicate the early stages of infection in which lipolysis, the glyoxalate cycle, and gluconeogenesis are thought to be critical metabolic requirements (Solomon et al., 2004a). The in planta library was designed to reveal both plant and fungal genes expressed at a late stage of infection. After trimming and removal of plant ESTs and alignment to the genome assembly, the in planta library formed 1448 and the oleate library formed 1231 unigenes (see Supplemental Data Set 2 online). Only 427 of the unigenes were found in both libraries. Although this represents 19% of the unigenes, it encompasses 46% of the ESTs, showing the genes expressed uniquely in one library are of relatively low expression.

The unigenes obtained from the in planta and oleate libraries were classified according to gene ontology (GO) categories. GO matches were obtained for 851 (59%) of the unigenes found in

the in planta and 736 (59%) of those found in the oleate library. Relative numbers of ESTs and genes in different GO classes were compared (Table 3). GO categories were ranked by statistical discrimination between the two libraries, and the top 10 are shown for each of biological process, cellular component, and molecular function.

Coexpression of fungal gene clusters responsible for the synthesis of secondary metabolites (Bok and Keller, 2004) and pathogenicity (Kamper et al., 2006) has been observed. We compared the number of ESTs found in the in planta and oleate libraries to search for clusters of coexpressed genes. Using a window of 10 contiguous genes, we scanned for regions with biased ratios of ESTs from either library. One putatively in planta-induced region stood out. These six genes, SNOG_16151.2 to SNOG_16157.2, were exclusively in the in planta library with 4, 20, 0, 4 10, and 1 EST clones, respectively. The genes have best hits to a major facilitator superfamily transporter, a phytanoyl-CoA dioxygenase, a CocE/NonD hydrolase, and a salicylate hydroxylase and are next to a transcription factor. Such a cluster may be involved in the degradation of phytols, phenylpropanoids, and catechols either for nutritional purposes, providing trichloroacetic acid intermediates via the β -ketoacid pathway or to detoxify wheat defense compound(s). It is intriguing that overexpression of the thiolase in the β -ketoacid pathway in *L. maculans* markedly reduced pathogenicity (Elliott and Howlett, 2006). Experiments to test these ideas in *S. nodorum* are in progress.

DISCUSSION

The estimated genome size of *S. nodorum* is 37.2 Mbp, which is significantly larger than the 28 to 32 Mbp previously estimated by pulsed-field gel analysis (Cooley and Caten, 1991). Electrophoretic karyotypes have proven to be unreliable estimators of total genome size in many fungal species (Orbach et al., 1988; Orbach, 1989; Talbot et al., 1993). In the case of *S. nodorum*, this discrepancy may be a consequence of comigration of chromosomal bands on pulsed-field gels leading to an underestimation of genome size (Cooley and Caten, 1991). The electrophoretic karyotype was found to be highly variable between strains, even when isolated from a single ascus, consistent with the generalization that many fungal species have plastic genome structures (Zolan, 1995). The revised genome size estimate is comparable to other sequenced filamentous fungi, such as the rice pathogen *M. grisea*, which is currently estimated to be 41.6 Mbp, and the nonpathogen *Neurospora crassa* now estimated at 39.2 Mbp.

Phylogenetic Analysis

The genome sequence has confirmed the phylogenetic placement of *S. nodorum* in the class Dothideomycetes. Along with the Eurotiomycetes (containing *Aspergillus* and human pathogens such as *Histoplasma*), Lecanoromycetes (the majority of the lichenized species), Leotiomyces (containing numerous endophytes and the plant pathogen *Sclerotinia*), and Sordariomycetes (with *Neurospora*, *Magnaporthe*, and *Colletotrichum* spp), the Dothideomycetes is now recognized as a major clade of the filamentous Ascomycota (James et al., 2006). Phylogenetic

analyses of full fungal genomes and large-scale taxon sampling agree with the placement of *S. nodorum* and point to the rapid divergence of these major classes of ascomycetes (Robbertse et al., 2006; Spatafora et al., 2006). The tree in Figure 2 is a focused sampling of the largest classes of the Ascomycota with an emphasis on plant pathogenic species and those with genome sequences. The Dothideomycetes is supported as a single class and represented by samples of five of the nine currently proposed orders (Eriksson, 2006; Schoch et al., 2006). *S. nodorum* is placed in the Pleosporales, a large order containing >100 genera and several thousand species, many of which are important plant pathogens. The Pleosporaceae family contains *Alternaria*, *Cochliobolus*, and *Pyrenophora* (Kodsueb et al., 2006) and is closely related to the clade containing the genera *Leptosphaeria* and *Phaeosphaeria* (*Stagonospora*). Other orders in the Dothideomycetes include the Dothideales and the Capnodiales (Schoch et al., 2006), which contains the pathogen genera *Mycosphaerella* and *Cladosporium*.

Repeated Elements in the Nuclear Genome

Prior to this study, only one unpublished study had been made of repetitive elements in the *S. nodorum* genome (Rawson, 2000). The de novo analysis of repeats is likely to become a feature of future genome sequencing projects as organisms with little prior molecular work are selected. The total amount of repetitive DNA in the *S. nodorum* nuclear genome is estimated at 4.5%. This compares with 9.5% in *M. grisea*. Some of these repeats could be associated with telomeres. Between 19 and 38 copies of telomere-associated repeats were found in the assembly. These numbers accord well with the 14 to 19 chromosomes visualized by pulsed-field electrophoresis (Cooley and Caten, 1991).

Studies of *S. nodorum* life cycle have indicated that it undergoes regular sexual crossing, particularly in areas with Mediterranean-style climates with the associated need to over-summer as ascospores (Bathgate and Loughman, 2001; Stukenbrock et al., 2006). The relatively low content of repetitive DNA is consistent with this observation. The prevalence of clear cases of RIP further confirms that meiosis is a frequent event. RIP has been found to varying degrees in other fungal genomes. It is notable that the closely related *L. maculans* has previously been shown experimentally to exhibit RIP (Idnurm and Howlett, 2003).

The Mitochondrial Genome

A distinctive feature of fungal mitochondrial genomes is the clustering of tRNA genes (Ghikas et al., 2006), and it is thought that both the tRNA gene content and their placement will be conserved in fungi (Table 4). The 27 tRNA genes clustered into five groups, with the two larger tRNA gene clusters flanking *ml*, a pattern common to other fungal mitochondrial DNAs (mtDNAs) (Tambor et al., 2006). The tRNA gene cluster 5' to *ml* had GDS¹WIS²P as a consensus, with its closest sequenced relative *M. graminicola* (GenBank accession number EU090238), while the 3'-downstream consensus was EAFLQHM, having many tRNA genes in the same order found in other Ascomycetes. Variation in the order of tRNAs, such as inversions in *Epidermophyton floccosum* (Ile-Trp) or in *Podospira anserina* and *S.*

Table 3. Comparison of GO Classification of Unigene and Transcript Numbers between the in Planta and Oleate Libraries

Biological Processes					
GO Identifier	Description	Loci	In Planta	Oleate	P Value ^a
Upregulated in planta					
GO:0006412	Protein biosynthesis	128	710	325	5.97E-19
GO:0045493	Xylan catabolism	24	31	0	6.16E-09
GO:0006508	Proteolysis	78	110	39	8.29E-07
GO:0008643	Carbohydrate transport	58	22	0	1.26E-06
GO:0000272	Polysaccharide catabolism	12	24	1	4.29E-06
GO:0016068	Type I hypersensitivity	13	87	31	9.67E-06
GO:0030245	Cellulose catabolism	16	18	0	1.33E-05
GO:0005975	Carbohydrate metabolism	102	53	16	6.57E-05
GO:0042732	D-xylose metabolism	2	25	4	2.01E-04
GO:0009051	Pentose-phosphate shunt, oxidative branch	2	21	3	4.07E-04
Upregulated oleate					
GO:0007582	Physiological process	24	8	48	1.04E-10
GO:0006629	Lipid metabolism	20	6	40	1.42E-09
GO:0006096	Glycolysis	21	42	92	5.93E-09
GO:0006108	Malate metabolism	4	12	45	5.48E-08
GO:0006099	Tricarboxylic acid cycle	20	50	85	4.11E-06
GO:0015986	ATP synthesis coupled proton transport	26	34	65	6.56E-06
GO:0006183	GTP biosynthesis	1	0	13	1.54E-05
GO:0006228	UTP biosynthesis	1	0	13	1.54E-05
GO:0006241	CTP biosynthesis	1	0	13	1.54E-05
GO:0006334	Nucleosome assembly	12	65	95	3.21E-05
Cellular Components					
GO Identifier	Description	Loci	In Planta	Oleate	P Value ^a
Upregulated in planta					
GO:0005840	Ribosome	89	567	262	3.14E-15
GO:0015935	Small ribosomal subunit	11	93	33	4.86E-06
GO:0005576	Extracellular region	36	23	1	7.44E-06
GO:0005730	Nucleolus	6	23	2	4.15E-05
GO:0030529	Ribonucleoprotein complex	25	60	19	4.31E-05
GO:0030125	Claathrin vesicle coat	9	7	0	8.86E-03
GO:0016020	Membrane	338	127	122	1.07E-02
GO:0016021	Integral to membrane	401	243	213	1.38E-02
GO:0019867	Outer membrane	7	45	24	1.40E-02
GO:0005874	Microtubule	19	8	1	1.97E-02
Upregulated oleate					
GO:0005829	Cytosol	34	19	50	1.01E-06
GO:0016469	Proton-transporting two-sector ATPase complex	24	27	60	1.41E-06
GO:0000786	Nucleosome	11	65	95	3.21E-05
GO:0043234	Protein complex	33	15	29	1.23E-03
GO:0005739	Mitochondrion	102	138	147	1.62E-03
GO:0005634	Nucleus	288	183	186	1.90E-03
GO:0005777	Peroxisome	14	26	38	3.39E-03
GO:0005746	Mitochondrial electron transport chain	8	36	47	4.40E-03
GO:0045261	Proton-transporting ATP synthase complex, catalytic core F(1)	5	14	23	7.49E-03
GO:0005778	Peroxisomal membrane	3	1	7	8.63E-03
Molecular Functions					
GO Identifier	Description	Loci	In Planta	Oleate	P Value ^a
Upregulated in planta					
GO:0003735	Structural constituent of ribosome	111	709	328	2.09E-18
GO:0004553	Hydrolase activity, hydrolyzing O-glycosyl compounds	83	55	5	4.13E-10
GO:0004252	Ser-type endopeptidase activity	14	43	3	6.92E-09
GO:0005351	Sugar porter activity	64	22	0	1.26E-06
GO:0046556	α -N-arabinofuranosidase activity	6	19	0	7.39E-06

(Continued)

Table 3. (continued).

Molecular Functions		Loci	In Planta	Oleate	P Value ^a
GO Identifier	Description				
GO:0030248	Cellulose binding	19	18	0	1.33E-05
GO:0004029	Aldehyde dehydrogenase (NAD) activity	1	15	0	7.85E-05
GO:0050661	NADP binding	6	23	3	1.60E-04
GO:0004185	Ser carboxypeptidase activity	8	13	0	2.56E-04
GO:0004616	Phosphogluconate dehydrogenase (decarboxylating) activity	4	22	3	2.56E-04
Upregulated oleate					
GO:0004459	L-lactate dehydrogenase activity	2	5	44	2.07E-11
GO:0030060	L-malate dehydrogenase activity	2	5	44	2.07E-11
GO:0005498	Sterol carrier activity	3	7	46	1.02E-10
GO:0008415	Acyltransferase activity	17	4	34	4.64E-09
GO:0005506	Iron ion binding	91	89	128	3.72E-06
GO:0004550	Nucleoside diphosphate kinase activity	1	0	13	1.54E-05
GO:0005554	Molecular function unknown	49	40	65	7.95E-05
GO:0046933	Hydrogen-transporting ATP synthase activity, rotational mechanism	24	34	58	8.73E-05
GO:0046961	Hydrogen-transporting atpase activity, rotational mechanism	24	34	58	8.73E-05
GO:0050660	FAD binding	27	13	30	2.85E-04

^aProbability of significant difference between the libraries (Audic and Claverie, 1997).

nodorum (Met-His), suggest that rearrangements are common in fungal mtDNAs (Table 4).

Kouvelis et al. (2004) argued that gene pairs *nad2-nad3*, *nad1-nad4*, *atp6-atp8*, and *cytb-cox1* would remain joined in ascomycetes with some possible exceptions, as already detected in *M. graminicola* that present only two of these gene pairs coupled. In *S. nodorum*, the *atp8-9* genes were not present, *cytb-cox1* were uncoupled, and the *nad1* and *nad4* genes were on sections of the mtDNA in an inverted orientation. Two *orfs* (*orf1* and *orf2*) had homologous sequences in the in planta EST library. While the *M. graminicola* mtDNA genome had no introns, four intron-encoded genes were found in *S. nodorum*, with high homology to LAGLIDADG-type endonucleases or GIY-YIG-type nucleases (see Supplemental Table 1 online). Intron-encoded proteins have also been reported in *P. anserina* (Cummings et al., 1990) and *Penicillium marneffeii* (Woo et al., 2003).

Functional Analysis of Proteins

Our primary goal in obtaining the genome sequence was to reveal genes likely to be involved in pathogenicity. While some genes seem to be specifically associated with pathogenicity in a single organism, other genes and gene families have been generally associated with pathogenicity, albeit they are also found in nonpathogens (see <http://www.phi-base.org/about.php>; Baldwin et al., 2006). Some of the generic functions are listed (Table 5; see Supplemental Data Set 2 and Supplemental Table 2 online). EST support was found for 59 of the genes, with no statistically significant difference in the numbers of ESTs in the in planta and oleate libraries.

Nonribosomal peptide synthetases (NRPSs) are modular enzymes that synthesize a diverse set of secondary metabolites, including the dothideomycete host-specific toxins AM-toxin, HC-toxin, and victorin from *Alternaria* and *Cochliobolus* species (Wolpert et al., 2002). NRPS genes from *C. heterostrophus* have

been analyzed in detail (Lee et al., 2005). Comparison of both protein sequences and domain structure of the *C. heterostrophus* NRPS genes (*NPS1-11*) with the eight identified in *S. nodorum* was undertaken (Table 6). Putative orthology was determined by identifying reciprocal best hits among the gene sets. Three pairs were identified. SNOG_02134.2 was linked to *NPS2*, and both appear to be orthologous to the *Aspergillus nidulans* gene *SidC* (Eisendle et al., 2003), which is responsible for the synthesis of ferricrocin, an intracellular iron storage and transport compound involved in protection against iron toxicity (Eisendle et al., 2006). It is likely that SNOG_02134.2 and *NPS2* play similar roles. SNOG_14638.2 was linked to *NPS6*, a ubiquitous gene with a related role in siderophore-mediated iron uptake and oxidative stress protection (Oide et al., 2006). Third, SNOG_14834.2 appears to be directly related to *NPS4*, *Psy1* from *Alternaria brassicae* (Guillemette et al., 2004), and *NPS2* from *Alternaria brassicicola* (Kim et al., 2007). Ab *NPS2* mutants are reduced in virulence, and the gene is predicted to encode a component of the conidial wall. It is likely that SNOG_14834.2 will have a similar generic role. Reciprocal best-hit relationships were observed between a further two SNOG NRPS genes and other fungal genes; SNOG_09081.2 was related to *PesA* (Bailey et al., 1996) and SNOG_14908.2 to the *Salps2* gene from *Hypocrea lixii* (Vizcaino et al., 2006). These genes plus SNOG_14834.2, SNOG_09488.2, and SNOG_01105.2 are all closely related to *NPS4*, suggesting that this five-gene subfamily is expanded in *S. nodorum*. Interestingly, a further seven NRPS genes from *C. heterostrophus* (*NPS3*, 5, 8, 10, 11, and 12) have no obvious ortholog in *S. nodorum*, suggesting expansion of this subfamily in the maize pathogen (Yoder and Turgeon, 2001). Intensive studies in *C. heterostrophus* showed that individual gene knockouts produced altered phenotypes only for *NPS6* (Lee et al., 2005), indicating redundancy of function. The smaller complement of NRPS genes in *M. grisea* (eight) and *S. nodorum* indicate that these organisms may be more fruitful models to study NRPS

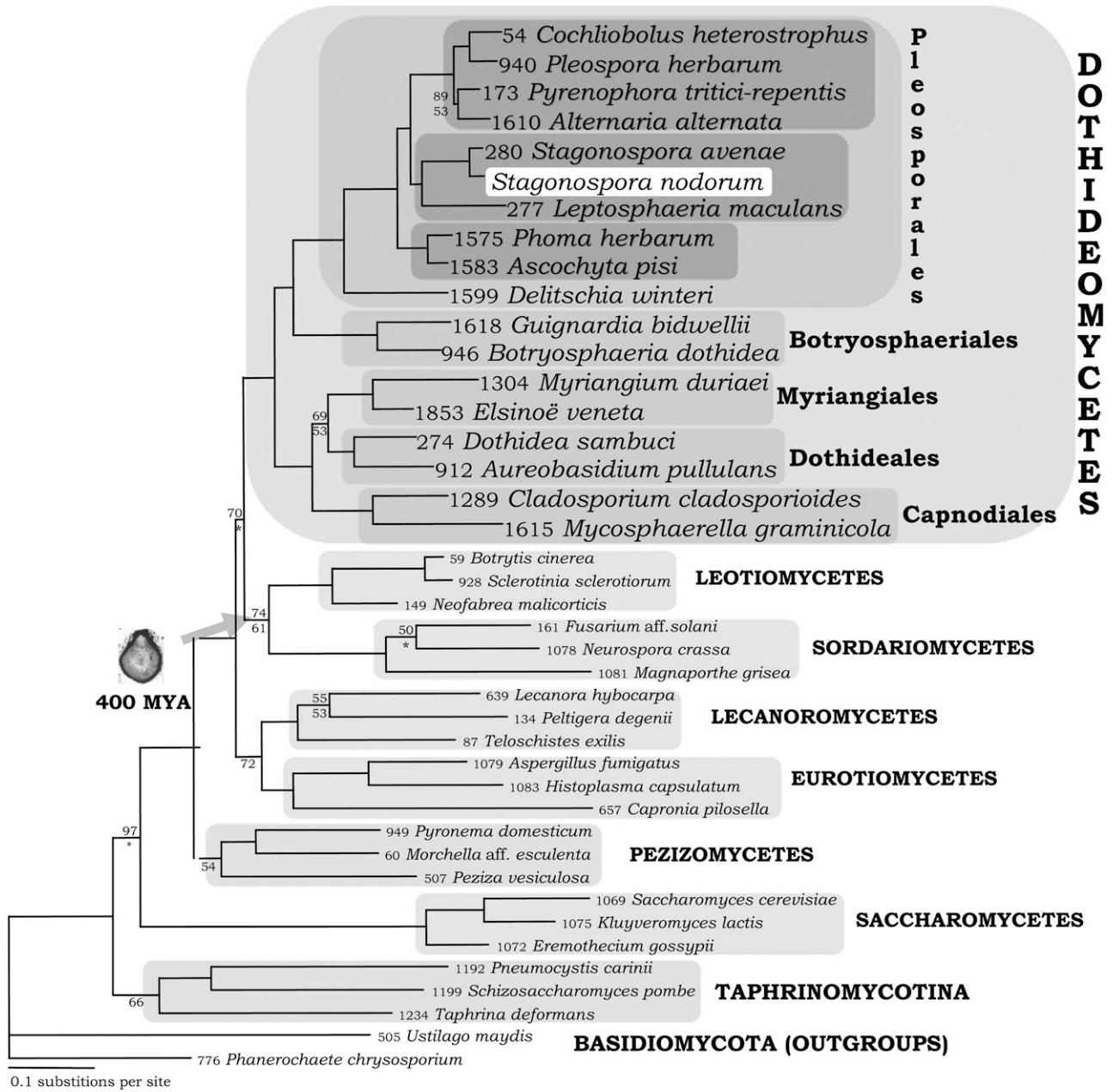


Figure 2. Phylogeny of Ascomycota Focused on Dothideomycetes.

Each species name is preceded by a unique AFTOL ID number (www.aftol.org). The tree is a 50% majority rule consensus tree of 45,000 trees obtained by Bayesian inference. All nodes had posterior probabilities of 100% except where numbers are shown above nodes. Similarly, all nodes had maximum likelihood bootstraps above 80% except where numbers are shown below nodes. Asterisks indicate nodes that were not resolved in >50% of bootstrap trees. Alignment data are provided in Supplemental Data Set 3 online. The gene data used are listed in Supplemental Table 3 online.

Table 4. Comparison of tRNA Gene Clusters Flanking the *rnl* Gene of the mtDNA Genome in Several Ascomycetes^a

Organism	5'-Upstream Region ^b	<i>rnl</i>	3'-Downstream Region ^b	Accession Number
<i>P. marneffeii</i>	RKG ¹ G ² DS ¹ WIS ² P	<i>rnl</i>	TEVM ¹ M ² L ¹ AFL ² QM ³ H	AY347307
<i>A. niger</i>	KGDS ¹ WIS ² P	<i>rnl</i>	TEVM ¹ M ² L ¹ AFL ² QM ³ H	DQ217399
<i>M. graminicola</i>	GDS ¹ WIS ² P	<i>rnl</i>	M ¹ L ¹ EAF ² YQM ² HRM ³	EU090238
<i>S. nodorum</i>	VKGDS ¹ WIRS ² P	<i>rnl</i>	T M ¹ M ² EAF ² LQHM ³	EU053989
<i>E. floccosum</i>	KGDSIWSP	<i>rnl</i>	TEVM ¹ M ² L ¹ AFL ² QM ³ H	AY916130
<i>H. jecorina</i>	ISWP	<i>rnl</i>	TEM ¹ M ² L ¹ AFKL ² QHM ³	AF447590
<i>P. anserina</i>	ISP	<i>rnl</i>	TEIM ¹ L ¹ AFL ² QHM ²	X55026

^a The tRNA gene order of listed organisms is based on GenBank sequences.

^b Capital letters refer to tRNA genes for the following: R, Arg; K, Lys; G, Gly; D, Asp; S, serine; W, Trp; I, Ile; P, Pro; T, Thr; E, Glu; V, Val; L, Leu; A, Ala; F, Phe; Q, Gln; H, His; Y, Tyr.

The numbers (1 to 3) indicate the presence of more tRNA genes for the same amino acid in the consensus sequence.

function. Furthermore, although toxins have been implicated in the virulence of both pathogens, nonribosomal synthetases cannot be expected to be a major source. No ESTs were found corresponding to these genes. This may be due to their large size or to a generally low level of expression.

Polyketide synthases (PKSs) are a second modular gene family strongly associated with pathogenicity (Kroken et al., 2003; Gaffoor et al., 2005), being responsible for the production of T-toxin from *C. heterostrophus* and PM-toxin from *Mycosphaerella zea-maydis* (Yun et al., 1998; Baker et al., 2006). *S. nodorum* is predicted to contain 19 PKS genes compared with the 24, 14, and 24 in the pathogens *M. grisea*, *Fusarium graminearum*, and *C. heterostrophus*, respectively, and 28 in the saprobe *A. nidulans* but significantly more than the seven in *N. crassa* (Table 5). Orthology relationships between the well-studied *F. graminearum* and *C. heterostrophus* gene sets and *S. nodorum* are shown in Table 7. Reciprocal best BLAST hits were observed with eight genes from *C. heterostrophus* and five from *F. graminearum*. This close relationship, particularly with *C. heterostrophus*, reflects the close phylogenetic relationship and suggests an ancient origin for the majority of the PKS

paralogs (Kroken et al., 2003). SNOG_11981.2 is supported by five ESTs from the in planta library and none from the oleate library, consistent with upregulation during infection and sporulation (no other PKSs have EST support). This gene is orthologous to nonreducing clade 2 PKS genes that are associated with 1,8-dihydroxynaphthalene melanin biosynthesis in *Bipolaris oryzae* and many other pathogens (Kroken et al., 2003; Moriwaki et al., 2004; Amnuaykanjanasin et al., 2005). We showed previously that *S. nodorum* produces melanin from dihydroxyphenylalanine (Solomon et al., 2004b), for which a PKS would not be necessary. This finding suggests that either *S. nodorum* produces 1,8-dihydroxynaphthalene melanin in addition to dihydroxyphenylalanine melanin or that SNOG_11981.2 plays another role.

A single PKS-NRPS hybrid protein (SNOG_00308.2) was identified in the genome of *S. nodorum* as was found for *F. graminearum* (Gaffoor et al., 2005) and *C. heterostrophus* (Lee et al., 2005). *C. heterostrophus* NPS7 and SNOG_00308.2 do not appear to be closely related, and it is likely that they evolved independently. By contrast, the hybrid protein of *F. graminearum* (Gz *FUS1*/FG12100) is closely related to SNOG_00308.2.

Table 5. Comparison of Selected Gene Families Identified by PFAM (Release 21) Domains between *S. nodorum* and Latest BROAD Releases of *M. grisea*, *N. crassa*, and *A. nidulans* and Incomplete Data from *C. heterostrophus* and *F. graminearum* (Kroken et al., 2003; Gaffoor et al., 2005; Lee et al., 2005)

Gene Family	<i>S. nodorum</i>				<i>M. grisea</i> Release 5	<i>N. crassa</i> v3 Assembly 7	<i>A. nidulans</i> Release 3	<i>C. heterostrophus</i> or <i>F. graminearum</i>
	Genes with PFAM Match	Genes with EST Clones	In Planta Clones	Oleate Clones				
G-alpha	4	2	3	0	3	3	3	
Cfem	4	1	17	15	9	6	4	9 Ch 8 Fg
Rhodopsin	2	2	14	8	1	2	1	
Hydrophobin class 1	0	0	0	0	1	1	3	
Hydrophobin class 2	2	0	0	0	2	1	0	
Feruloyl esterase	8	0	0	0	10	1	5	
Cutinase	11	4	4	8	16	3	4	
Subtilisin	11	3	8	2	26	6	3	
Transcription factor	94	25	37	43	97	83	195	
Cytochrome p450	103	20	27	20	115	39	102	
PKS	19	1	3	0	24	7	28	24 Ch 14 Fg
NRPS	8	1	1	0	8	3	13	10 Ch
PKS-NRPS	1	0	0	0	7	0	0	1 Ch

Table 6. Potential Orthologs to *S. nodorum* NRPS Genes

SN15 NRPS	Domain/ Module Structure ^a	Best Hit	Accession Number	Organism	Reciprocal ^b	Percentage of Similarity ^c	Domain/Module Structure ^d	Inferred Function
SNOG_01105.2	TCyAT/CATE/ CAT/CAT	<i>NPS4</i>	AAX09986	<i>C. heterostrophus</i>	No	37.2%	TECAT/CATE/ CAT/CATE/C/T/C/T	Unknown
		Abre <i>Psy1</i>	AAP78735	<i>A. brassicae</i>	No	39.0%	TECAT/CATE/CAT/ CATE/C/T/C/T	
SNOG_02134.2	AT/CAT/CAT/ C/T/C	<i>NPS2</i>	AAX09984	<i>C. heterostrophus</i>	Yes	53.8%	AT/CAT/CAT/CATT/C	Iron uptake and oxidative stress protection
		<i>SidC</i>	AAP56239	<i>A. nidulans</i>	Yes	40.3%	A/CA/CA/C/T/C	
SNOG_07021.2	ATCT	<i>NPS1</i>	AAX09983	<i>C. heterostrophus</i>	No	13.8%	AT/CAMT/CAT/C	Unknown
		<i>PesA</i>	CAA61605	<i>Metarhizium anisopliae</i>	No	10.2%	ATE/CAT/CAT/CATE/C	Unknown
SNOG_09081.2	ATE/CAT/CAT/ CAT/C	<i>NPS4</i>	AAX09986	<i>C. heterostrophus</i>	No	33.0%	TECAT/CATE/CAT/ CATE/C/T/C/T	Unknown
		<i>PesA</i>	CAA61605	<i>M. anisopliae</i>	Yes	58.1%	ATE/CAT/CAT/CATE/C	Unknown
SNOG_09488.2	CATE/CAT/ CATE	<i>NPS4</i>	AAX09986	<i>C. heterostrophus</i>	No	26.3%	TECAT/CATE/CAT/ CATE/C/T/C/T	Unknown
		<i>PesA</i>	CAA61605	<i>M. anisopliae</i>	No	36.6%	ATE/CAT/CAT/CATE/C	Unknown
SNOG_14098.2	ATE/CAT/CAT/ CATE/C	<i>NPS4</i>	AAX09986	<i>C. heterostrophus</i>	No	32.3%	TECAT/CATE/CAT/ CATE/C/T/C/T	Unknown
		<i>Salps2</i>	CAI38799	<i>Hypocrea lixii</i>	Yes	34.4%	TCAT/CAT/CAT	
SNOG_14368.2	AT/C/TT	<i>NPS6</i>	AAX09988	<i>C. heterostrophus</i>	Yes	73.5%	AT/C/AT	Virulence, siderophore- mediated iron metabolism, tolerance to oxidative stress
		<i>NPS6</i>	ABI51982	<i>C. miyabeanus</i>	Yes	73.5%	AT/C/TT	
SNOG_14834.2	TECAT/CATE/ CAT/CATE/C	<i>NPS4</i>	AAX09986	<i>C. heterostrophus</i>	Yes	75.9%	TECAT/CATE/CAT/ CATE/C/T/C/T	Virulence, conidial cell wall construction, spore germination/ sporulation efficiency
		Ab <i>NPS2^e</i>		<i>A. brassicicola</i>	Yes	78.2%	TECAT/CATE/CAT/ CATE/C/T/C	
		Abre <i>Psy1</i>	AAP78735	<i>A. brassicae</i>	Yes	78.0%	TECAT/CATE/CAT/ CATE/C/T/C/T	

^a Domain abbreviations: A, adenylation; C, condensation; Cy, Cyclization; E, epimerization; T, thiolation; Te, Thioesterase. Potential orthologs were identified by best BLASTP hits to NRPS genes in *C. heterostrophus* (Lee et al., 2005) and by best informative hit to the nonredundant database at NCBI of e-value $<1 \times 10^{-10}$.

^b The best hit of the identified gene in the *S. nodorum* gene set was observed reciprocally.

^c Percentage of similarity of ortholog pairs (Needleman and Wunsch, 1970) via NEEDLE (Rice et al., 2000).

^d Domain structure and modular organization for all sequences was determined via the online NRPS-PKS database (Ansari et al., 2004). It should be noted that domain structure predictions may vary slightly from those stated in the original studies.

^e Protein sequence for Ab *NPS2* available in Supplemental Appendix S2 online from Kim et al. (2007).

Overall, they are 54.5% similar, and apart from an acyl binding domain found only in SNOG_00308.2, the domain structures are identical. Gz *FUS1* produces fusarin C, a mycotoxin (Gaffoor et al., 2005). The best hit (with 59.4% similarity) to SNOG_00308.2 in *M. grisea* is *Ace1*, a hybrid PKS/NRPS that confers avirulence to *M. grisea* during rice (*Oryza sativa*) infection (Bohnert et al., 2004). It will be intriguing to determine if the product of SNOG_00308.2 is required for pathogenicity.

G-alpha proteins have been extensively studied in fungi (Lafon et al., 2006), and many are required for pathogenicity. Distinct roles for three g-alpha genes have been revealed in *M. grisea*, *A. nidulans*, and *N. crassa*. It was therefore a surprise to find a fourth g-alpha gene in the *S. nodorum* genome. This gene

(SNOG_06158.2) was shown to be expressed in vitro and in planta. It was investigated by gene disruption, and its loss resulted in no discernable phenotype (data not shown). A fourth g-alpha protein has been recently identified in both *A. oryzae* (Lafon et al., 2006) and *Ustilago maydis* (Kamper et al., 2006), but neither shows significant sequence similarity to that of *S. nodorum*. Indeed, SNOG_06158.2 is most similar to *Gba3* among the *U. maydis* g-alphas and *GpaB* among the *A. oryzae* genes.

G-alpha proteins transduce extracellular signals leading to infection-specific development (Solomon et al., 2004b). *Pth11* and *AC11* are two *M. grisea* genes encoding transmembrane receptors that defined a new protein domain, CFEM (Kulkarni et al., 2003), with roles in g-protein signaling. *M. grisea* has nine

Table 7. Potential Orthologs of *S. nodorum* PKS Genes

SN15 PKS	Domain/Module Structure	Best Hit	Accession Number	Organism	Reciprocal Similarity	Inferred Clade	Domain/Module Structure	Inferred Function of Ortholog	
SNOG_00477.2	KsAtKrAcp	fg12100		<i>F. graminearum</i>	No	21.6%	Fungal 6MSAS	KsAtAcp/KrAcp/Acp KsAtKrAcp	6-Methylsalicylic acid synthesis (Fujii et al., 1996)
		PKS25	AAR90279	<i>C. heterostrophus</i>	Yes	59.7%			
		atX	BAA20102	<i>A. terreus</i>	Yes	69.0%			
SNOG_02561.2	KsAtErKrAcp	fg12109		<i>F. graminearum</i>	No	42.1%	Reducing PKS clade I	KsAtErKrAcp KsAtErKrAcp KsAtDhErKrAcp	Synthesis of diketide moiety of compactin or similar polyketide (Abe et al., 2002a, 2002b)
		PKS3	AAR90258	<i>C. heterostrophus</i>	Yes	45.8%			
		mlcB	BAC20566	<i>P. citrinum</i>	Yes	47.7%			
SNOG_04868.2	KsAtErKrAcp	fg05794		<i>F. graminearum</i>	Yes	38.9%	Reducing PKS clade I	KsAtAcp/ErKrAcp KsAtErKr	Synthesis of squalestatin (Nicholson et al., 2001)
		PKS6	AAR90261	<i>C. heterostrophus</i>	No	46.5%			
		type I PKS	AAO62426	<i>Phoma</i> sp C2932	No	49.8%			
SNOG_05791.2	KsAtErKrAcp	fg12109		<i>F. graminearum</i>	Yes	43.1%	Reducing PKS clade I	KsAtErKrAcp KsAtErKr	Synthesis of alternapyrone (Fujii et al., 2005)
		PKS5	AAR90261	<i>C. heterostrophus</i>	Yes	73.1%			
		atl5	BAD83684	<i>A. solani</i>	Yes	79.2%			
SNOG_06676.2	KsAtErKr	fg01790		<i>F. graminearum</i>	No	31.3%	Reducing PKS clade IV	KsAtErKrAcp KsAtErKr	Synthesis of fumonisin (Proctor et al., 1999)
		PKS14	AAR92221	<i>G. moniliformis</i>	No	31.8%			
		FUM1	AAD43562	<i>G. moniliformis</i>	No	30.0%			
SNOG_06682.1	KsAtAcp	fg03964		<i>F. graminearum</i>	No	36.2%	Nonreducing PKS clade III (uncharacterized)	KsAtAcp KsAtAcp	Synthesis of citrinin (Shimizu et al., 2005)
		PKS17	AAR90253	<i>B. fuckeliana</i>	Yes	43.9%			
		pksCT	BAD44749	<i>M. purpureus</i>	Yes	44.7%			
SNOG_07866.2	KsAtKr	fg12100		<i>F. graminearum</i>	No	37.8%	Reducing PKS clade II	KsAtAcp/KrAcp/Acp KsAtKr	Synthesis of polyketide similar to citrinin/lovastatin
		PKS16	AAR90270	<i>C. heterostrophus</i>	Yes	67.9%			
		EqiS	AAV66106	<i>F. heterosporum</i>	Yes	39.8%			
SNOG_08274.2	KsAcp/AtAcp/Acp	fg12040		<i>F. graminearum</i>	No	40.3%	Nonreducing PKS clade II (e.g., melanins)	KsAtAcp KsAtAcp/Acp KsAtAcp/Acp	Synthesis of perithecial pigment, autofusarin, or similar polyketide (Graziani et al., 2004)
		PKS12	AAR90248	<i>B. fuckeliana</i>	No	44.5%			
		PKS	AAS48892	<i>N. haematococca</i>	No	47.8%			
SNOG_08614.2	KsAtAcp/Acp/Te	fg12125		<i>F. graminearum</i>	Yes	41.2%	Nonreducing PKS clade I	KsAtAcp/Acp KsAtAcp/Acp KsAtAcp/Acp	Synthesis of perithecial pigment, cercosporin, or similar polyketide; cercosporin is a reactive oxygen species-generating toxin degrading plant cell membranes (Chung et al., 2003)
		PKS3	AAR92210	<i>G. moniliformis</i>	No	49.3%			
		PKS	AAT69682	<i>C. nicotianae</i>	No	60.7%			
SNOG_09623.2	KsAtAcp/ErKrAcp	fg01790		<i>F. graminearum</i>	No	58.9%	Reducing PKS clade IV	KsAtErKrAcp KsAtErKrAcp KsAtErKrAcp	Synthesis of fumonisin (Proctor et al., 1999)
		PKS11	AAR90266	<i>C. heterostrophus</i>	Yes	56.1%			
		FUM1	AAD43562	<i>G. moniliformis</i>	Yes	57.7%			
SNOG_11066.2	KsKsAtErKrAcp	fg12055		<i>F. graminearum</i>	No	43.2%	Reducing PKS clade III	KsAtErKrAcp KsAtErKrAcp KsAtErKrAcp	High virulence; synthesis of T-toxin; zearalenone (Gaffoor et al., 2005; Baker et al., 2006)
		PKS8	AAR90244	<i>B. fuckeliana</i>	Yes	59.7%			
		PKS2	ABB76806	<i>C. heterostrophus</i>	Yes	44.9%			
SNOG_11076.2	KsAtDhErKrAcp	fg01790		<i>F. graminearum</i>	Yes	62.8%	Reducing PKS clade IV	KsAtErKrAcp KsAtDhErKrAcp	Synthesis of fumonisin (Proctor et al., 1999)
		PKS14	AAR90268	<i>C. heterostrophus</i>	Yes	82.7%			
		FUM1	AAD43562	<i>G. moniliformis</i>	No	53.9%			
SNOG_11272.2	KsKsAtErKrAcp	fg12055		<i>F. graminearum</i>	No	44.7%	Reducing PKS clade IV	KsAtErKrAcp KsAtErKr	Synthesis of zearalenone or similar polyketide; similar to HR-type PKS (Gaffoor et al., 2005)
		PKS14	AAR92221	<i>G. moniliformis</i>	Yes	48.7%			
		PKSKA1	AAY32931	<i>Xylaria</i> sp BCC 1067	No	47.3%			
SNOG_11981.2	KsAtAcp/Acp/Acp/Te	fg12040		<i>F. graminearum</i>	Yes	54.9%	Nonreducing PKS clade II	KsAtAcp KsAtAcp/Acp/Te KsAtAcp/Acp/Te	Synthesis of melanin (Moriwaki et al., 2004; Amnuaykanjanasin et al., 2005).
		PKS18	AAR90272	<i>C. heterostrophus</i>	Yes	85.7%			
		PKS1	BAD22832	<i>B. oryzae</i>	Yes	88.2%			
SNOG_12897.2	KsAtErKr	fg10548		<i>F. graminearum</i>	No	39.7%	Reducing PKS clade I	KsAtErKrAcp KsAtAcp/ErKrAcp KsAtErKrAcp	Synthesis of alternapyrone (Fujii et al., 2005)
		PKS5	AAR92212	<i>G. moniliformis</i>	No	38.2%			
		alt5	BAD83684	<i>A. solani</i>	No	37.8%			
SNOG_13032.2	KsAtAcpKr	fg01790		<i>F. graminearum</i>	No	40.4%	Reducing PKS clade IV	KsAtErKrAcp KsAtAcp/Acp/ErKrAcp KsAtErKrAcp	Synthesis of fumonisin (Proctor et al., 1999)
		PKS12	AAR92219	<i>G. moniliformis</i>	No	45.1%			
		FUM1	AAD43562	<i>G. moniliformis</i>	No	39.1%			
SNOG_14927.2	KsAtDhKrAcp	fg01790		<i>F. graminearum</i>	No	44.3%	Reducing PKS clade IV	KsAtErKrAcp KsAtAcp/ErKrAcp KsAtDhErKrAcp	Synthesis of diketide moiety of compactin (Abe et al., 2002a, 2002b).
		PKS15	AAR90269	<i>C. heterostrophus</i>	No	43.5%			
		PKS	BAC20566	<i>P. citrinum</i>	No	39.1%			

(Continued)

Table 7. (continued).

SN15 PKS	Domain/Module Structure	Best Hit	Accession Number	Organism	Reciprocal	Similarity	Inferred Clade	Domain/Module Structure	Inferred Function of Ortholog
SNOG_15829.2	KsAtAcp	fg12040		<i>F. graminearum</i>	No	42.2%	Nonreducing PKS proteins basal to clades I and II (uncharacterized)	KsAtAcp	Synthesis of melanin, autofusarin, or similar polyketide (Moriwaki et al., 2004)
		PKS1	BAD22832	<i>B. oryzae</i>	No	41.3%		KsAtAcp/Acp/Te	
		PKS14	AAR90250	<i>B. fuckeliana</i>	No	67.6%		KsAtAcp/Acp	
SNOG_15965.2	KsAtErKrAcp	fg10548		<i>F. graminearum</i>	No	43.9%	Reducing PKS clade IV	KsAtErKrAcp	Synthesis of fumonisin (Proctor et al., 1999)
		PKS10	AAR90246	<i>B. fuckeliana</i>	Yes	68.8%		KsAtErKrAcp	
		PKSKA1	AAY32931	<i>Xylaria</i> sp BCC 1067	No	54.7%		KsAtErKrAcp	

Domain abbreviations: ACP, acyl-carrier protein domain; At, acetyl transferase; Dh, dehydratase; Er, enoyl reductase; Kr, keto reductase; Ks, keto synthase; Te, thioesterase. Potential orthologs to PKSs *C. heterostrophus* and *F. graminearum* (Kroken et al., 2003; Gaffoor et al., 2005) and by best informative hit to the nonredundant database at NCBI of e-value $<1 \times 10^{-10}$. Domain structure and modular organization for all sequences was determined via the online NRPS-PKS database (Ansari et al., 2004). It should be noted that domain structure predictions may vary slightly from those stated in the original studies. Percentage of similarity of ortholog pairs was determined (Needleman and Wunsch, 1970) via NEEDLE (Rice et al., 2000).

CFEM domain proteins, and *F. graminearum* has eight. Using a combination of domain searches and BLAST searches seeded with the *M. grisea* and *F. graminearum* genes, we identified six related genes (Table 8). Four of these have at least a weak match to the CFEM domain, but only three are predicted to be transmembrane proteins. SNOG_09610.2 appears to be the ortholog of *Pth11* and the *F. graminearum* gene fg05821, suggesting these genes are ancient and conserved. *Pth11* is required for appressorial development and perception of suitable surfaces (DeZwaan et al., 1999). Neither *S. nodorum* nor *F. graminearum* form classical appressoria (Solomon et al., 2006b), suggesting that the genes have different functions in these species. SNOG_05942.2 is also closely related to *Pth11*. Knockout strains for this gene were obtained but had no obvious phenotype (data not shown). SNOG_03589.2 is also related to *Pth11* and appears to be a transmembrane protein but lacks the CFEM domain. Both SNOG_08876.2 and SNOG_15007.2 possess CFEM domains and a signal peptide but do not appear to be integral membrane proteins. Knockout strains for SNOG_08876.2 were obtained but revealed no obvious phenotype (data not shown). SNOG_15007.2 is similar to glycosylphosphatidylinositol-anchored CFEM-containing proteins from three other fungal species. It appears to be heavily expressed both in the oleate and in planta EST libraries with 17 and 27 ESTs, respectively. A clear role for this gene is as yet unknown. CFEM domain proteins are thought to be involved in surface signal perception, and three candidates for this role have been identified. The paucity of such genes in *S. nodorum* and lack of phenotype associated with deletion of two of them suggests that this function may be covered by a different class of transmembrane receptors.

Hydrophobins are small, secreted proteins with eight Cys residues in a conserved pattern that coat the fungal mycelium and spore (Wessels, 1994). Class 2 hydrophobins are restricted to ascomycetes, whereas class 1 hydrophobins are also found in other fungal divisions (Linder et al., 2005). Two class 2 and no class 1 hydrophobin genes were found in the *S. nodorum* genome (see Supplemental Figure 1 online). This is an unusual example of an ascomycete genome with only class 2 hydrophobin genes. It is interesting to note that although a range of *Neurospora* species all contained a gene orthologous to the class 1 hydrophobin *EAS* gene from *N. crassa*, they were expressed significantly only in

species that produced aerial conidia (Winefield et al., 2007). *S. nodorum* produces pycnidiospores in a gelatinous cirrus adapted for rain dispersal (Solomon et al., 2006b). It may be that the absence of aerial mitospore production negates the need for class 1 hydrophobins.

Two rhodopsin-like genes were found in the genome, one of which is similar to the bacteriorhodopsin-like gene found in *L. maculans* that is a proton pump (Sumii et al., 2005). The likely physiological roles of these genes are currently under investigation.

The interaction between a pathogen and its host is to a large extent orchestrated by the proteins that are secreted or localized to the cell wall or cell membrane. Pathogens such as *M. grisea*, which kill and degrade host tissues, have been shown to secrete large numbers of degradative enzymes (Dean et al., 2005). More surprisingly, the biotrophic pathogen *U. maydis* was also found to secrete many proteins; many of the genes are clustered, coexpressed, and required for normal pathogenesis but are of unknown molecular functions (Kamper et al., 2006). We have therefore analyzed the putative proteome of *S. nodorum* for potentially secreted proteins and compared them with these pathogens and the saprobe *N. crassa*. A total of 1782 proteins was predicted to be extracellular based on predictions using WoLF PSORT; a further 1760 were predicted to be plasma membrane located (see Supplemental Data Set 2 online). GO annotations were assigned via Blast2GO for 551 of the putatively extracellular proteins (Table 9). They are dominated by carbohydrate and protein degradation enzymes as would be expected and which is consistent with the EST analysis (see below). The role of many fungal extracellular proteins is currently unknown. Among the *S. nodorum* predicted extracellular proteins, 1231 had no GO annotation. Of these, only 410 had significant matches to putatively extracellular proteins from *U. maydis*, *M. grisea*, or *N. crassa* (Figure 3). More of these 410 genes had homologs in *M. grisea* (13 + 91 = 104) than in *N. crassa* (3 + 39 = 42). As *M. grisea* and *N. crassa* are phylogenetically equidistant from *S. nodorum*, this suggests both that the pathogens secrete more proteins than *N. crassa* and that the genes are related. Expanding this generalization will require genome analysis of a saprobic dothideomycete. A further 251 genes (89 + 162) had homologs in both *M. grisea* and *N. crassa*. Another 118 *S. nodorum* putatively

Table 8. Potential Orthologs of *S. nodorum* CFEM Proteins Identified by Matches to PFAM Domain PF05730 and Best Hit to *M. grisea* and *F. graminearum* CFEM Proteins

Best Seed ^a	Similarity	SN15 CFEM Protein	PF05730 Match ^a	Location ^b	7tm ^c	Informative Best Hit (Nonredundant)	Reciprocal	Similarity	Inferred Function
fg08554	36.4%	SNOG_02161.2	No	Extracellular	No	None			Unknown
		SNOG_08876.2	Yes	Extracellular	No	None			Unknown
MGG06724.5	21.4%	SNOG_03589.2	No	Plasma membrane	Yes	AAD30437 <i>M. grisea</i> PTH11	No	24.8%	GPCR involved in surface perception
MGG05871.5	38.3%	SNOG_05942.2	Yes	Plasma membrane	Yes	AAD30438 <i>M. grisea</i> PTH11	No	38.3%	GPCR involved in surface perception
MGG10473.5	57.5%	SNOG_09610.2	Yes	Plasma membrane	Yes	AAD30437 <i>M. grisea</i> PTH11	Yes	33.1%	GPCR involved in surface perception
						Fg05821	Yes	59.0%	
MGG05531.5	38.0%	SNOG_15007.2	Yes	Extracellular	No	ABA33784 Pro-rich antigen-like protein (<i>Paracoccidioides brasiliensis</i>)	Yes	51.2%	Similar to Pro-rich antigens and Ag2/Pra CRoW domains more commonly identified as immunoreactive antigens
						XP_750946.1 GPI-anchored CFEM domain protein (<i>Aspergillus fumigatus</i> Af293)	Yes	56.6%	antigens of mammalian fungal pathogens (Peng et al., 2002);
						AAP84613.1 Ag2/Pra CRoW domain (<i>Coccidioides posadasii</i>)	Yes	25.7%	similar to GPI-anchored CFEM proteins

^a In addition to HMMER matches to PFAM accession PF05730 (using gathering cutoffs), CFEM domain-containing proteins from *M. grisea* (BROAD release 5: MGG_01149.5, MGG_01872.5, MGG_05531.5, MGG_05871.5, MGG_06724.5, MGG_06755.5, MGG_07005.5, MGG_09570.5, and MGG_10473.5) and *Fusarium graminearum* (FGDB: fg00588, fg02077, fg02155, fg02374, fg03897, fg05175, fg05821, and fg08554) were used as seeds to identify putative CFEM proteins by their best BLASTP match with an e-value $< 1 \times 10^{-10}$ to *S. nodorum*.

^{b,c} Cellular location was determined with WoLF PSORT (Horton et al., 2007), and the presence of transmembrane-spanning regions (7tm) was determined by consensus between TMHMM (Krogh et al., 2001), TMPRED (Hofmann and Stoffel, 1993), and Phobius (Kall et al., 2004). Best hits of *Stagonospora* CFEM proteins to the nonredundant protein database at NCBI was determined by informative BLASTP hits of e-value $< 1 \times 10^{-10}$ (hits excluding seed and self hits, which are not hypothetical or unknown and preferentially yield useful functional information).

secreted genes of unknown function had significant similarity to genes encoding the *U. maydis* secretome, including 13 that uniquely hit the biotrophic basidiomycete. We found no obvious patterns of clustering of any of these secreted genes. The most striking finding was that 821 genes had no significant similarity to predicted extracellular proteins of any of these fully sequenced genomes. These large numbers of putatively secreted proteins of mostly unknown functions, whose genes appear to be rapidly evolving, points to a hitherto unsuspected complexity and subtlety in the interaction between the pathogen and its environments.

One newly recognized aspect of *S. nodorum* is the production of secreted proteinaceous toxins. SNOG_16571.2 encodes a host-specific protein toxin called ToxA that determines the interaction with the dominant wheat disease susceptibility gene *Tsn1* (Friesen et al., 2006; Liu et al., 2006). Population genetic evidence suggests that this gene was interspecifically trans-

ferred to the wheat tan spot pathogen, *P. tritici-repentis*, prior to 1941, thereby converting a minor into a major pathogen. An RGD motif that is involved in import into susceptible plant cells is required for activity (Meinhardt et al., 2002; Manning et al., 2004; Manning and Ciuffetti, 2005). Biochemical and genetic evidence suggests that *S. nodorum* isolates contain several other proteinaceous toxins (Liu et al., 2004a, 2004b). ToxA is a 13.2-kD protein, and current research indicates that the other toxins are also small proteins. Among the predicted extracellular proteins, 840 are < 30 kD and 26 have an RGD motif (see Supplemental Data Set 2 online). Analysis of these toxin candidates is underway.

Gene Expression during Infection

When analyzed by biological process and molecular function, the in planta EST library was dominated by genes involved in the

Table 9. The Most Abundant Gene Ontologies Associated with the Predicted Secretome

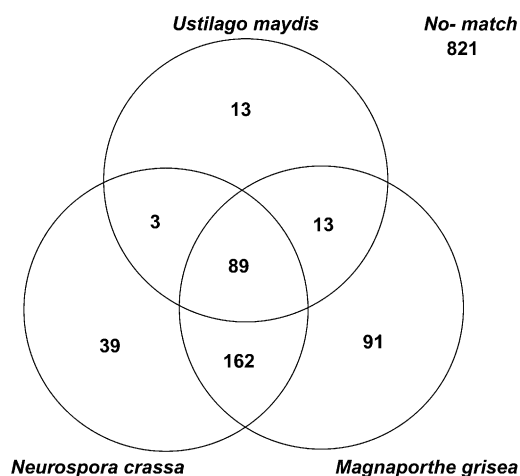
GO Identifier	Description	Genes
Biological processes		
GO:0005975	Carbohydrate metabolism	42
GO:0008152	Metabolism	34
GO:0006118	Electron transport	30
GO:0006508	Proteolysis	26
GO:0045493	Xylan catabolism	19
GO:0044237	Cellular metabolism	17
GO:0030245	Cellulose catabolism	12
GO:0000272	Polysaccharide catabolism	10
Molecular functions		
GO:0003674	Molecular function	68
GO:0016491	Oxidoreductase activity	52
GO:0016787	Hydrolase activity	52
GO:0004553	Hydrolase activity, hydrolyzing O-glycosyl compounds	48
GO:0005488	Binding	34
GO:0003824	Catalytic activity	33
GO:0046872	Metal ion binding	19
GO:0030248	Cellulose binding	18
GO:0016798	Hydrolase activity, acting on glycosyl bonds	13
GO:0008233	Peptidase activity	12
GO:0008810	Cellulase activity	12
GO:0016740	Transferase activity	12
GO:0016789	Carboxylic ester hydrolase activity	10

biosynthesis of proteins and in the degradation and use of extracellular proteins and carbohydrates, specifically cellulose and arabino-xylan (Table 3; see Supplemental Table 5 online). The secretion of proteases (Bindschedler et al., 2003), xylanases, and cellulases suggests that the fungus catabolizes plant proteins and carbohydrates for energy in planta at this late stage of infection. Studies in a range of pathogens suggest that early infection is characterized by the catabolism of internal lipid stores and that mid stages are characterized by the use of external sugars and amino acids (Solomon et al., 2003a). These studies of late infection suggest that polymerized substrates are used after the more easily available substrates are exhausted and provide a novel perspective to in planta nutrition. The abundance of transcripts linked to protein synthesis indicates that this process is very active during this stage of infection and may be related to the massive secretion of degradative enzymes and to the synthesis of proteins needed for sporulation. A similar picture was observed when the genes were analyzed by cellular component (Table 3) with gene products destined for the ribosome dominating. Genes whose products are targeted to the nucleolus and cytoskeleton illustrate the importance of nuclear division and cytokinesis at this stage of infection as many new cell types are elaborated in the developing pycnidium. Thirty-six gene products targeted to the extracellular region include a protease, an α -glucuronidase, and various glucanases consistent with the picture of polymerized substrate breakdown.

Late-stage infection has rarely been examined in plant–fungal interactions, and it is therefore noteworthy that upregulation of

transcripts involved in protein synthesis was also observed in late-stage infections of wheat by *M. graminicola* (Keon et al., 2005). The high rate of protein synthesis may be required for pycnidial biogenesis and may also represent an attractive target for fungicidal intervention.

The oleate EST library was dominated by genes involved in lipid and malate metabolism, the trichloroacetic acid cycle, and electron transport. To determine whether the ratio of ESTs in the in planta and oleate libraries was indicative of early- and late-stage infection, transcript levels from eight candidate genes were determined by a quantitative PCR. The genes were chosen from those found exclusively in the in planta library. Transcripts were quantified in cDNA pools made from RNA isolated from in vitro and in planta growth of SN15 at early and late infection time points. The in vitro cultures sampled at 4 DAI did not contain any pycnidia, whereas cultures sampled at 18 DAI were heavily sporulating with many pycnidia. To isolate RNA from both early and late infections of wheat, an SN15 infection latent period assay was used to provide in planta infection transcripts (Solomon et al., 2003b). Lesions were excised after 8 and 12 DAI, representing early and late infection stages. The three genes most upregulated during growth in planta (SNOG_00557.2, SNOG_03877.2, and SNOG_16499.2) all had >20 in planta ESTs, indicating that the EST frequencies were useful predictors of gene expression at these levels. SNOG_00557.2 was the gene with the highest peak expression level in planta and the largest difference between in vitro and in planta conditions. As the gene is predicted to be an arabinofuranosidase, this reaffirmed the important role of carbohydrases during colonization of the host tissue. Overall, the four tissue types represented clear states of nonsporulation and sporulation during both in vitro and in planta growth. All the genes were found to be expressed in the 12-DAI infected sample, and this was the highest level observed in all but

**Figure 3.** Homology Relationships of the *S. nodorum* Secretome.

The 1231 predicted extracellular proteins without GO annotation were compared with the latest releases of the *U. maydis*, *N. crassa*, and *M. grisea* genomes. Counts are best hits of e-value <1e-10 if predicted as extracellular by WoLF PSORT.

one case (see Supplemental Figure 2 online). On the other hand, moderate to high levels of gene expression were found in the in vitro samples from six of the eight genes. Attempts to use axenic samples to mimic infection has a long history (Coleman et al., 1997; Talbot et al., 1997; Solomon et al., 2003a; Trail et al., 2003; Thomma et al., 2006). Our data indicate that oleate feeding is not a significantly closer model for infection than starvation has proved to be.

Genome Architecture

Colinearity of gene order is a notable feature of closely related plant and animal genomes but is represented in fungi by a complex pattern of dispersed colinearity, such as observed between *Aspergillus* spp (Galagan et al., 2005). This low degree of organizational conservation can be attributed to the 200 million year separation of these species and the rarity of meiotic events that would tend to maintain chromosomal integrity. *S. nodorum* is the first dothideomycete to have its sequence publicly released; thus, the closest species for which whole-genome comparisons could be made are the Aspergilli and *N. crassa*, which are separated from *S. nodorum* by ~400 million years of evolution. Thus far, we have been unable to detect significant regions of colinearity with other sequenced genomes, but it is possible that more sensitive methods and the release of more closely related genome sequences will succeed in revealing patterns of chromosomal level evolution.

At a smaller scale, the mating type loci of *L. maculans*, *C. heterostrophus*, *A. alternata*, and *M. graminicola* have been previously analyzed (Cozijnsen and Howlett, 2003). Apart from *Mat1-1* and *orf1*, the only shared genes were a DNA ligase gene found in *L. maculans* and *M. graminicola* and *Gap1* found in

L. maculans and *C. heterostrophus*. The colinearity between *L. maculans* and *S. nodorum* is more complete. Figure 4A shows the relationship of gene order and orientation between these sibling species. It is clear that gene order and orientation are conserved, though the intergenic regions have no discernable relationships. This confirms the close phylogenetic relationship between these species, with *S. nodorum* closest to *L. maculans* and more distantly related to *C. heterostrophus*.

There is tantalizing evidence of residual colinearity of the genes present in a contiguous 38-kb region of *L. maculans* DNA (Idnurm et al., 2003). Six of the nine *L. maculans* genes have orthologs within a 200-kb region of *S. nodorum* DNA. Gene orientation is retained, but they are interspersed with ~60 other predicted genes (Figure 4B).

A different pattern of colinearity is apparent in the quinate gene cluster. The quinate genes regulate the catabolism of quinate and have a wide distribution in filamentous fungi (Giles et al., 1991). The cluster comprises seven coregulated genes. In some cases, portions of the cluster are repeated at other genomic locations. In *S. nodorum*, the main cluster is located on scaffold 19 with two genes on scaffold 12. Figure 5 show the relationship of gene content and order in six fungal species. As the species for comparison span 400 million years of evolution, it is apparent that clustering of these genes per se is highly conserved. However, the gene order and orientation shows no conservation apart from the constant juxtaposition of homologs of Qa-1S and Qa1-F and of Qa-X and Qa-2. Even in these cases, though, some are 5' to 5' and others are 3' to 3'. It appears, therefore, that there must be selection for retention of clustering of these seven genes, even if the exact orientation may not be so important. It may be that such proximity clustering is important in that it enables gene regulation by chromatin remodeling mediated by a

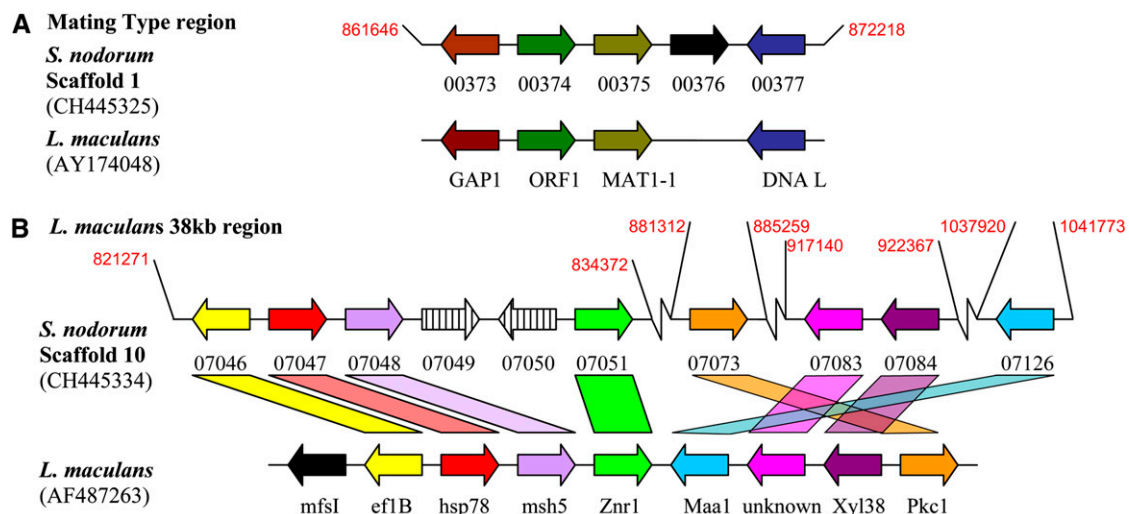


Figure 4. Colinearity between *S. nodorum* SN15 and *L. maculans* Identified by tBLASTX.

(A) Mating-type locus.

(B) A 38-kb region of *L. maculans*.

Colors indicate an orthologous relationship between genes, whereas black indicates no relationship. Numbers in red give coordinates on the *S. nodorum* scaffolds.

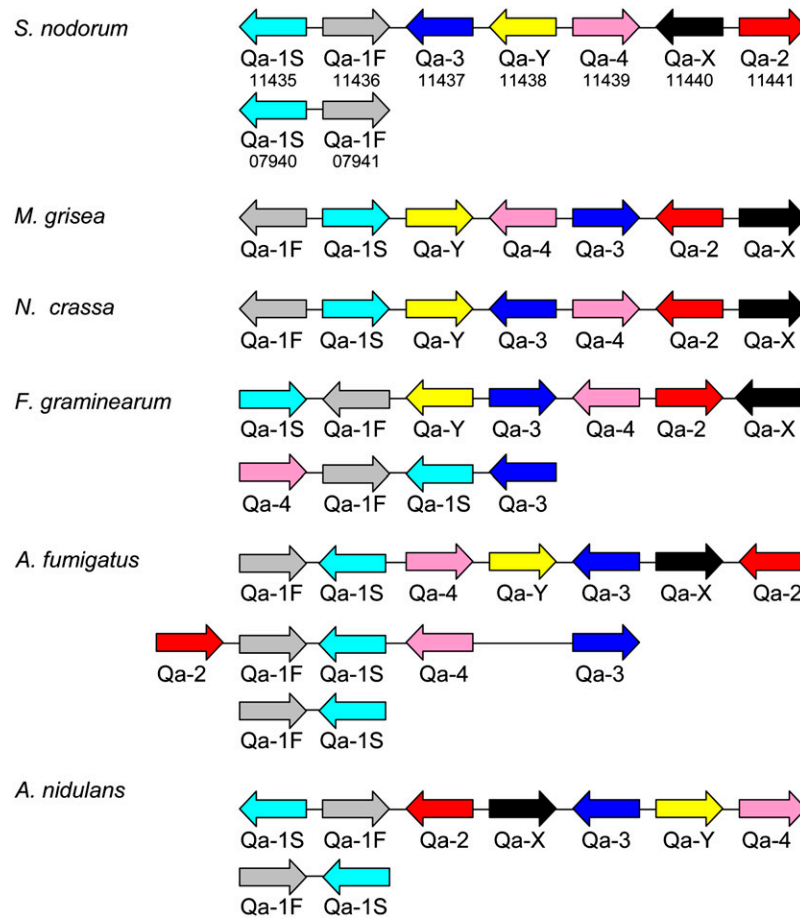


Figure 5. Organization of the Quinate Cluster from Several Sequenced Fungal Genomes.

Numbers under the *S. nodorum* genes refer to the SNOG identifiers. The *S. nodorum* genes are located on scaffolds 19 and 12, respectively.

gene such as *LaeA* (Bok and Keller, 2004). SNOG_11365.2 is an apparent ortholog of *LaeA*.

Fungi have a truly ancient history, many times longer than that of animals and flowering plants (Padovan et al., 2005). The extent of genetic diversity is correspondingly large. Phylogenetic analysis of fungi has been hampered by a paucity of reliable morphological indicators. As a consequence, phylogenetic reconstruction of the fungi has been particularly unstable until the widespread introduction of multigene-based DNA sequence comparisons. This study confirms the overall monophyletic characters of the Dothideomycetes and the Pleosporales taxa. These groups contain many thousands of species and are notable for their content of major plant pathogens infecting many important plant families. The origins of this class, likely >400 million years ago, is considerably older than their plant hosts. It is particularly interesting to note that all the fungal plant pathogens that are well established as host-specific toxin producers are in this class (*Stagonospora*, *Cochliobolus*, *Pyrenophora*, *M. zeae-maydis*, and *Alternaria*). Taken as a whole, the pathogens in this class are mainly described as necrotrophic, while a few are debatably described as biotrophic (*Venturia* and *C. fulvum*) or hemibiotrophic (*L. maculans*, *M. graminicola*, and *M. fijiensis*). None of the

species in this class are obligate pathogens, and none possess classical haustoria (Oliver and Ipcho, 2004); furthermore, many other species are nonpathogenic. The genome sequence of *S. nodorum* represents an important point of comparison from which to derive hypotheses about the genetic basis of pathogenicity in these organisms. Genome sequences of several of these species are in progress (Goodwin, 2004), including *A. brassicicola*, *M. fijiensis*, *M. graminicola*, *L. maculans*, and *P. tritici-repentis*, or have been completed but not released (*C. heterostrophus*; Catlett et al., 2003). Three of these species, *S. nodorum*, *M. graminicola*, and *P. tritici-repentis*, are wheat pathogens. The possibility of multiple pairwise comparisons of gene content between phylogenetically and ecologically close species promises to be a powerful method to derive workably small lists of candidate effector genes controlling pathogenicity, host specificity, and life cycle characters and thus provide ideas for the generation of novel crop protection strategies. The genome sequence provides the tools for global transcriptome analysis, thereby identifying the genes expressed during different phases of infection. This study has also highlighted secreted proteins, which appear to be markedly more numerous than in nonpathogens but which have predominately mysterious roles. Finally, the

genome sequence is an essential prerequisite for the critical analysis of hypotheses of interspecific gene transfer. This has already been identified in pathogens in general (Richards et al., 2006) and *S. nodorum* in particular (Friesen et al., 2006; Stukenbrock and McDonald, 2007) and may emerge as a major feature in the evolution of these organisms.

METHODS

Fungal Strains

Stagonospora nodorum strain SN15 (Solomon et al., 2003b) was used for both genome and EST libraries and has been deposited at the Fungal Genetics Stock Center. The genome sequence was obtained as described (http://www.broad.mit.edu/annotation/genome/stagonospora_nodorum/Assembly.html). The sequences are available for download from GenBank under accession number AAGI00000000.

Phylogenetic Analysis

A combined matrix of 41 taxa was generated from DNA sequences obtained from two ribosomal (nuclear large and small subunit [nuc-LSU and nuc-SSU]) and three protein genes (elongation factor 1 α [EF-1 α] and the largest and second largest subunits of RNA polymerase II [*RPB1* and *RPB2*]). Data were obtained from the Assembling the Fungal Tree of Life (AFTOL; www.aftol.org) and GenBank sequence databases, which aligned in ClustalX (Thompson et al., 1997) and manually improved where necessary. After introns and ambiguously aligned characters were excluded, 6694 bp were used in the final analyses. In some cases, genes were missing (see Supplemental Table 3 and Supplemental Data Set 3 online). The resulting data were combined and delimited into 11 partitions, including nuc-SSU, nuc-LSU, and the first, second, and third codon positions of EF-1 α , *RPB1*, and *RPB2*, with unique models applied to each partition. Metropolis coupled Markov chain Monte Carlo analyses were conducted using MrBayes 3.1.2 (Huelsenbeck and Ronquist, 2001) with a six-parameter model of evolution (generalized time reversible) (Rodriguez et al., 1990) and gamma distribution approximated with four categories and a proportion of invariable sites. Trees were sampled every 100th generation for 5,000,000 generations. Three runs were completed to ensure that stationarity was reached, and 5000 trees were discarded as "burn in" for each. Posterior probabilities were determined by calculating a 50% majority-rule consensus tree of 45,000 trees from a single run. Maximum likelihood bootstrap proportions were calculated by doing 1000 replicates in RAxML-VI-HPC (Stamatakis, 2006) with the GTRCAT model approximation and 25 rate categories with the same data partitions as for the Bayesian runs.

Repetitive Elements

Repetitive elements were identified de novo using RepeatScout v1.0.0 (Price et al., 2005) with a minimum threshold of 10 matches and a minimum repeat length of 200 bp. Newly generated repeats were aligned to the genome assembly via BLASTN v2.0 (Altschul et al., 1990). Hits were discarded if sequence identity fell below 35% or alignment length was <200 bp. For each repeat, the number of filtered hits was counted, and repeats were discarded if the number of hits to the assembly was <10. Prototype repeat regions were defined by identification of sequence similarities among themselves via BLASTN and deletion of redundant repeat sequence. Regions of the genome assembly that matched to a repeat were aligned using MUSCLE v3.6 (Edgar, 2004). To identify repeat type and function, repeats were compared with the nonredundant sequence database hosted by NCBI via BLASTN/BLASTX, and subrepeat regions within repeats were also analyzed. Tandem repeats were identified

using Tandem Repeat Finder (Benson, 1999), direct repeats were identified via MegaBLAST (Zhang et al., 2000), and inverted repeats were identified using both MegaBLAST and eINVERTED (Rice et al., 2000).

Putative telomeric regions were predicted by considering scaffold ends containing successive repetitive elements without interspersed predicted protein coding genes. The occurrence of repeat classes within these regions was counted and compared with occurrences throughout the genome. Where >85% of the repeats were found to be at nongenic scaffold end regions, these classes were classified as telomeric repeats. The scaffold ends were predicted to be physical telomeres if they contained three or more telomeric repeats.

To analyze and compare the prevalence of RIP mutation, we developed a program to compare RIP mutations between multiple sequences (J.K. Hane and R.P. Oliver, unpublished data). RIPCAL compares the aligned sequences against a designated model sequence (in this case the trimmed de novo repeats) and was configured to calculate RIP (Dean et al., 2005).

Gene Content

An automated genome annotation was initially created using the Calhoun annotation system. A combination of gene prediction programs, FGENESH, FGENESH+, and GENEID, and 317 manually curated transcripts were used. GENEWISE was used with non-species specific parameters to predict genes from proteins identified by BLASTX. To refine the initial genome annotation, a further 10,752 EST reads were obtained from an EST library from oleate-grown mycelium and 10,751 from *S. nodorum*-infected wheat (see below for details). These EST sequences were screened against a library of wheat ESTs, trimmed for vector sequence manually, for poly(A) tail sequence using TrimEST (Rice et al., 2000), screened for unusable sequences of poor quality, filtered for remaining sequence of ≥ 50 bp, and aligned to the genome assembly using Sim4 (Florea et al., 1998). ESTs with multiple genomic locations were assigned their optimum location based on percent identity, total alignment length, and best location of the EST mated pair. Gene models were manually annotated according to optimum EST alignments using Apollo (Lewis et al., 2002).

Genes that were fully supported by EST data were used to train the gene prediction program UNVEIL (Majoros et al., 2003). Second-round gene annotations were created by combining gene predictions with EST data, with EST data replacing predicted gene models, and UNVEIL predictions preferred over first-round predictions. Genes with coding regions <50 amino acids were discarded. The numerical identifiers assigned during the first-round predictions have been retained. New gene models were assigned loci from 20,000 onwards. Updated loci (UNVEIL and EST supported) have been given the numerical suffix 2 (e.g., SNOG_16571.2). The 5354 unsupported genes have retained the numerical identifiers and suffix 1. Where genic regions lack EST support, only the coding sequence is reported.

ESTs not aligned to the assembly by Sim4 were compared with the unassembled reads via BLASTN. EST with matches to unassembled reads with an e-value of <1E-10 were clustered into contigs using cap3 (Huang and Madan, 1999). The assembled ESTs were tested for single open reading frames using getORF (Rice et al., 2000), and possible genes were determined by BLASTP (Altschul et al., 1990) to protein databases at NCBI. One new gene (STAG_20208.1) was identified by this method. We have chosen not to alter genes where gene models conflicted with homologs except where colinearity evidence confirms orthology (Figure 4). Updated files of gene and protein sequences are available from R. Oliver (roliver@murdoch.edu.au).

Proteins were assigned putative functional classes by searching for relevant PFAM (Bateman et al., 1999) domains (Bateman et al., 2004) with HMMER v2.0 (Eddy, 1998) (see Supplemental Data Set 2 and Supplemental Table 2 online). Putative gene ontology was assigned via BLASTP with BLAST2GO (Conesa et al., 2005). Due to the relatively poor

identification of certain PKS and NRPS domains using resources like PFAM (Bateman et al., 2004) and CD-SEARCH (Marchler-Bauer and Bryant, 2004; Marchler-Bauer et al., 2005), PKS and NRPS domains and their modular organization were further elucidated with online tools available at NRPS-PKS (Yadav et al., 2003; Ansari et al., 2004). Subcellular localization and secretion was predicted via WoLF PSORT (Horton et al., 2007).

EST Library Construction

For the construction of the in planta cDNA library, wheat (*Triticum aestivum*) cv Amery was infected with *S. nodorum* SN15 as a whole plant spray and processed as a latent period assay (Solomon et al., 2006b). Necrotic tissue was excised from the leaves at 10, 11, and 12 DAI for RNA isolation. RNA was isolated by the Trizol method (Sigma-Aldrich).

Material for the oleate library was generated as follows: minimal medium (100 mL) + sucrose (0.5% [w/v]) was inoculated with *S. nodorum* SN15 pycnidiospores (2.75×10^7) and incubated at 22°C with shaking (130 rpm) for 4 d. Mycelia was harvested, washed, and added to 100 mL of minimal media, including 0.05% (v/v) Tween 80 and 0.2% (w/v) oleate as the carbon source. The culture was incubated as before for 30 h before being harvested, washed, snap frozen in liquid nitrogen, and freeze-dried in a Maxi Dry Lyo (Heto Holten). mRNA was extracted using the MESSagemaker mRNA purification-cloning kit (Gibco/Invitrogen) according to manufacturer's instructions. A total of 2.3 µg of mRNA was used as template for reverse transcription to cDNA. The in planta cDNA library was constructed using the SMART cDNA library construction kit (Clontech), and the oleate library was constructed in pSPORT1 (Gibco/Invitrogen). All manipulations were performed according to the manufacturer's instructions. Phage DNA was packaged using the GigapackIII Gold phage packaging system (Stratagene) according to the manufacturer's instructions. Phages were grown, amplified, and mass-excised to bacterial clones according to the provided protocols. The final libraries were both estimated to contain ~500,000 clones.

Quantitative PCR

Total RNA (1 µg) was reverse transcribed to cDNA using iScript reverse transcriptase premix (Bio-Rad) according to the manufacturer's instructions. RNA from three biological replicates was pooled for a single cDNA synthesis. cDNA reactions were used as PCR template at 1:50 dilution for in vitro-grown SN15 samples and at 1:5 dilution for in planta-grown SN15 samples. Quantitative PCR reactions consisted of 10 µL of iQ SYBR green supermix (Bio-Rad), forward and reverse primers (each at 1.2 µM), and 5 µL of template DNA in a 20 µL reaction. Reactions were incubated in a Rotor-Gene 3000 thermocycler (Corbett Research). Cycling conditions were 3 min/95°C and then 35 cycles of 10 s/95°C, 20 s/57°C, and 72°C/20 s. Amplicon fluorescence from template of unknown concentration was compared with that from genomic DNA standards of 25, 2.5, 0.25, and 0.025 ng/reaction. All reactions were performed with two technical replicates. Data were analyzed using the Rotorgene software version 6.0 (Corbett Research). Primer sequences are listed in Supplemental Table 4 online.

Accession Number

Sequence data from this article can be found in the GenBank/EMBL data libraries under accession number AAGI00000000.

Supplemental Data

The following materials are available in the online version of this article.

Supplemental Figure 1. Aligned Kyte and Doolittle Hydrophobicity Plots.

Supplemental Figure 2. Quantitative PCR Analysis of Gene Expression from in Planta-Associated Genes.

Supplemental Table 1. Mitochondrial Genes.

Supplemental Table 2. Summary of PFAM Domains Used for Identification.

Supplemental Table 3. List of Species Used in This Study.

Supplemental Table 4. PCR Primers for Abundant in Planta-Associated Genes.

Supplemental Table 5. EST Data for Abundant in Planta-Associated Genes.

Supplemental Data Set 1. Repetitive Elements: Telomeres, Sub-repeats, and Similarity Scores.

Supplemental Data Set 2. Gene Summary.

Supplemental Data Set 3. Alignments for Figure 1 as a Non-interleaved Nexus Formatted Text File.

ACKNOWLEDGMENTS

Funding was provided by the Australian Grains Research and Development Corporation (UMU14; we particularly thank James Fortune, John Sandow, and John Lovett for their support of this project), by the Swiss Federal Institute of Technology Zurich, by the Swiss National Science Foundation (Grant 3100A0-104145), by MIT, and by the National Science Foundation (DEB-0228725; Assembling the Fungal Tree of Life). We thank Soeren Rasmussen for help with bioinformatics, Robert Lee for the oleate EST library, and Tim Friesen (USDA) for comments on the manuscript. We dedicate this article to the recently retired Chris Caten who has inspired our work on *S. nodorum*.

Received May 10, 2007; revised September 11, 2007; accepted October 15, 2007; published November 16, 2007.

REFERENCES

- Abe, Y., Suzuki, T., Mizuno, T., Ono, C., Iwamoto, K., Hosobuchi, M., and Yoshikawa, H. (2002b). Effect of increased dosage of the ML-236B (compactin) biosynthetic gene cluster on ML-236B production in *Penicillium citrinum*. *Mol. Genet. Genomics* **268**: 130–137.
- Abe, Y., Suzuki, T., Ono, C., Iwamoto, K., Hosobuchi, M., and Yoshikawa, H. (2002a). Molecular cloning and characterization of an ML-236B (compactin) biosynthetic gene cluster in *Penicillium citrinum*. *Mol. Genet. Genomics* **267**: 636–646.
- Agrios, G. (2005). *Plant Pathology*. (Burlington, MA: Elsevier Academic Press).
- Altschul, S.F., Gish, W., Miller, W., Myers, E.W., and Lipman, D.J. (1990). Basic local alignment search tool. *J. Mol. Biol.* **215**: 403–410.
- Amnuaykanjanasin, A., Punya, J., Paungmoung, P., Rungrod, A., Tachaleat, A., Pongpattanakitshote, S., Cheevadhanarak, S., and Tanticharoen, M. (2005). Diversity of type I polyketide synthase genes in the wood-decay fungus *Xylaria* sp. BCC 1067. *FEMS Microbiol. Lett.* **251**: 125–136.
- Ansari, M.Z., Yadav, G., Gokhale, R.S., and Mohanty, D. (2004). NRPS-PKS: A knowledge-based resource for analysis of NRPS/PKS megasynthases. *Nucleic Acids Res.* **32**: W405–413.
- Audic, S., and Claverie, J.M. (1997). The significance of digital gene expression profiles. *Genome Res.* **7**: 986–995.
- Bailey, A.M., Kershaw, M.J., Hunt, B.A., Paterson, I.C., Charnley, A.K., Reynolds, S.E., and Clarkson, J.M. (1996). Cloning and

- sequence analysis of an intron-containing domain from a peptide synthetase-encoding gene of the entomopathogenic fungus *Metarhizium anisopliae*. *Gene* **173**: 195–197.
- Baker, S.E., Kroken, S., Inderbitzin, P., Asvarak, T., Li, B.Y., Shi, L., Yoder, O.C., and Turgeon, B.G.** (2006). Two polyketide synthase-encoding genes are required for biosynthesis of the polyketide virulence factor, T-toxin, by *Cochliobolus heterostrophus*. *Mol. Plant Microbe Interact.* **19**: 139–149.
- Baldwin, T.K., Winnenburger, R., Urban, M., Rawlings, C., Koehler, J., and Hammond-Kosack, K.E.** (2006). The pathogen-host interactions database (PHI-base) provides insights into generic and novel themes of pathogenicity. *Mol. Plant Microbe Interact.* **19**: 1451–1462.
- Bateman, A., Birney, E., Durbin, R., Eddy, S.R., Finn, R.D., and Sonnhammer, E.L.** (1999). Pfam 3.1: 1313 multiple alignments and profile HMMs match the majority of proteins. *Nucleic Acids Res.* **27**: 260–262.
- Bateman, A., et al.** (2004). The Pfam protein families database. *Nucleic Acids Res.* **32**: D138–D141.
- Bathgate, J.A., and Loughman, R.** (2001). Ascospores are a source of inoculum of *Phaeosphaeria nodorum*, *P. avenaria f. sp. avenaria* and *Mycosphaerella graminicola* in Western Australia. *Australas. Plant Pathol.* **30**: 317–322.
- Bearchell, S.J., Fraaije, B.A., Shaw, M.W., and Fitt, B.D.L.** (2005). Wheat archive links long-term fungal pathogen population dynamics to air pollution. *Proc. Natl. Acad. Sci. USA* **102**: 5438–5442.
- Bennett, R.S., Yun, S.H., Lee, T.Y., Turgeon, B.G., Arseniuk, E., Cunfer, B.M., and Bergstrom, G.C.** (2003). Identity and conservation of mating type genes in geographically diverse isolates of *Phaeosphaeria nodorum*. *Fungal Genet. Biol.* **40**: 25–37.
- Benson, G.** (1999). Tandem repeats finder: A program to analyze DNA sequences. *Nucleic Acids Res.* **27**: 573–580.
- Bindschedler, L.V., Sanchez, P., Dunn, S., Mikan, J., Thangavelu, M., Clarkson, J.M., and Cooper, R.M.** (2003). Deletion of the SNP1 trypsin protease from *Stagonospora nodorum* reveals another major protease expressed during infection. *Fungal Genet. Biol.* **38**: 43–53.
- Bohnert, H.U., Fudal, I., Dioh, W., Tharreau, D., Notteghem, J.L., and Lebrun, M.H.** (2004). A putative polyketide synthase/peptide synthetase from *Magnaporthe grisea* signals pathogen attack to resistant rice. *Plant Cell* **16**: 2499–2513.
- Bok, J.W., and Keller, N.P.** (2004). LaeA, a regulator of secondary metabolism in *Aspergillus* spp. *Eukaryot. Cell* **3**: 527–535.
- Cambareri, E., Jensen, B., Schabtach, E., and Selker, E.** (1989). Repeat-induced G-C to A-T mutations in *Neurospora*. *Science* **244**: 1571–1575.
- Catlett, N.L., Yoder, O.C., and Turgeon, B.G.** (2003). Whole-genome analysis of two-component signal transduction genes in fungal pathogens. *Eukaryot. Cell* **2**: 1151–1161.
- Chung, K.R., Ehrenshaft, M., Wetzler, D.K., and Daub, M.E.** (2003). Cercosporin-deficient mutants by plasmid tagging in the asexual fungus *Cercospora nicotianae*. *Mol. Genet. Genomics* **270**: 103–113.
- Coleman, M., Henricot, B., Arnau, J., and Oliver, R.P.** (1997). Starvation-induced genes of the tomato pathogen *Cladosporium fulvum* are also induced during growth in planta. *Mol. Plant Microbe Interact.* **10**: 1106–1109.
- Conesa, A., Gotz, S., Garcia-Gomez, J.M., Terol, J., Talon, M., and Robles, M.** (2005). Blast2GO: A universal tool for annotation, visualization and analysis in functional genomics research. *Bioinformatics* **21**: 3674–3676.
- Cooley, R., Shaw, R., Franklin, F., and Caten, C.** (1988). Transformation of the phytopathogenic fungus *Septoria nodorum* to hygromycin B resistance. *Curr. Genet.* **13**: 383–386.
- Cooley, R.N., and Caten, C.E.** (1991). Variation in electrophoretic karyotype between strains of *Septoria nodorum*. *Mol. Gen. Genet.* **228**: 17–23.
- Cozijnsen, A.J., and Howlett, B.J.** (2003). Characterisation of the mating-type locus of the plant pathogenic ascomycete *Leptosphaeria maculans*. *Curr. Genet.* **43**: 351–357.
- Cummings, D., McNally, K., Domenico, J., and Matsuura, E.** (1990). The complete DNA sequence of the mitochondrial genome of *Podospora anserina*. *Curr. Genet.* **17**: 375–402.
- Dancer, J., Daniels, A., Cooley, N., and Foster, S.** (1999). *Septoria tritici* and *Stagonospora nodorum* as model pathogens for fungicide discovery. In *Septoria on Cereals: A Study of Pathosystems*, J.A. Lucas, P. Bowyer, and H.M. Anderson, eds (New York: ABI Publishing), pp. 316–331.
- Dean, R.A., et al.** (2005). The genome sequence of the rice blast fungus *Magnaporthe grisea*. *Nature* **434**: 980–986.
- Del Prado, R., Schmitt, I., Kautz, S., Palice, Z., Luecking, R., and Lumbsch, H.T.** (2006). Molecular data place Trypetheliaceae in Dothideomycetes. *Mycol. Res.* **110**: 511–520.
- DeZwaan, T.M., Carroll, A.M., Valent, B., and Sweigard, J.A.** (1999). *Magnaporthe grisea* pth11p is a novel plasma membrane protein that mediates appressorium differentiation in response to inductive substrate cues. *Plant Cell* **11**: 2013–2030.
- Eddy, S.R.** (1998). Profile hidden Markov models. *Bioinformatics* **14**: 755–763.
- Edgar, R.C.** (2004). MUSCLE: A multiple sequence alignment method with reduced time and space complexity. *BMC Bioinformatics* **5**: 113.
- Eisendle, M., Oberegger, H., Zadra, I., and Haas, H.** (2003). The siderophore system is essential for viability of *Aspergillus nidulans*: Functional analysis of two genes encoding l-ornithine N 5-monooxygenase (sidA) and a non-ribosomal peptide synthetase (sidC). *Mol. Microbiol.* **49**: 359–375.
- Eisendle, M., Schrettl, M., Kragl, C., Müller, D., Illmer, P., and Haas, H.** (2006). The intracellular siderophore ferricrocin is involved in iron storage, oxidative-stress resistance, germination, and sexual development in *Aspergillus nidulans*. *Eukaryot. Cell* **5**: 1596–1603.
- Elliott, C.E., and Howlett, B.J.** (2006). Overexpression of a 3-ketoacyl-CoA thiolase in *Leptosphaeria maculans* causes reduced pathogenicity on *Brassica napus*. *Mol. Plant Microbe Interact.* **19**: 588–596.
- Eriksson, O.E.** (2006). Outline of Ascomycota. *Mycotax* **12**: 1–82.
- Florea, L., Hartzell, G., Zhang, Z., Rubin, G.M., and Miller, W.** (1998). A computer program for aligning a cDNA sequence with a genomic DNA sequence. *Genome Res.* **8**: 967–974.
- Friesen, T.L., Stukenbrock, E.H., Liu, Z.H., Meinhardt, S., Ling, H., Faris, J.D., Rasmussen, J.B., Solomon, P.S., McDonald, B.A., and Oliver, R.P.** (2006). Emergence of a new disease as a result of interspecific virulence gene transfer. *Nat. Genet.* **38**: 953–956.
- Fujii, I., Ono, Y., Tada, H., Gomi, K., Ebizuka, Y., and Sankawa, U.** (1996). Cloning of the polyketide synthase gene atX from *Aspergillus terreus* and its identification as the 6-methylsalicylic acid synthase gene by heterologous expression. *Mol. Gen. Genet.* **253**: 1–10.
- Fujii, I., Yoshida, N., Shimomaki, S., Oikawa, H., and Ebizuka, Y.** (2005). An iterative type I polyketide synthase PKS catalyzes synthesis of the decaketide alternapyrone with regio-specific octamethylation. *Chem. Biol.* **12**: 1301–1309.
- Gaffoor, I., Brown, D., Plattner, R., Proctor, R., Qi, W., and Trail, F.** (2005). Functional analysis of the polyketide synthase genes in the filamentous fungus *Gibberella zeae* (anamorph *Fusarium graminearum*). *Eukaryot. Cell* **4**: 1926–1933.
- Galagan, J.E., et al.** (2003). The genome sequence of the filamentous fungus *Neurospora crassa*. *Nature* **422**: 859–868.
- Galagan, J.E., et al.** (2005). Sequencing of *Aspergillus nidulans* and comparative analysis with *A. fumigatus* and *A. oryzae*. *Nature* **438**: 1105–1115.
- Ghikas, D.V., Kouvelis, V.N., and Typas, M.A.** (2006). The complete mitochondrial genome of the entomopathogenic fungus *Metarhizium*

- anisopliae* var. *anisopliae*: Gene order and trn gene clusters reveal a common evolutionary course for all Sordariomycetes, while intergenic regions show variation. *Arch. Microbiol.* **185**: 393–401.
- Giles, N.H., Geever, R.F., Asch, D.K., Avalos, J., and Case, M.E.** (1991). Organization and regulation of the qa (quinic acid) genes in *Neurospora crassa* and other fungi. *J. Hered.* **82**: 1–7.
- Goodwin, S.B.** (2004). Minimum phylogenetic coverage: An additional criterion to guide the selection of microbial pathogens for initial genomic sequencing efforts. *Phytopathology* **94**: 800–804.
- Graziani, S., Vasnier, C., and Daboussi, M.J.** (2004). Novel polyketide synthase from *Nectria haematococca*. *Appl. Environ. Microbiol.* **70**: 2984–2988.
- Guillemette, T., Sellam, A., and Simoneau, P.** (2004). Analysis of a nonribosomal peptide synthetase gene from *Alternaria brassicae* and flanking genomic sequences. *Curr. Genet.* **45**: 214–224.
- Hofmann, K., and Stoffel, W.** (1993). TMbase - A database of membrane spanning proteins segments. *Biol. Chem. Hoppe Seyler* **374**: 166.
- Horton, P., Park, K.J., Obayashi, T., Fujita, N., Harada, H., Adams-Collier, C.J., and Nakai, K.** (2007). WoLF PSORT: Protein localization predictor. *Nucleic Acids Res.* **35**: W585–587.
- Huang, X., and Madan, A.** (1999). CAP3: A DNA sequence assembly program. *Genome Res.* **9**: 868–877.
- Huelsenbeck, J.P., and Ronquist, F.** (2001). MRBAYES: Bayesian inference of phylogenetic trees. *Bioinformatics* **17**: 754–755.
- Idnurm, A., and Howlett, B.J.** (2003). Analysis of loss of pathogenicity mutants reveals that repeat-induced point mutations can occur in the Dothideomycete *Leptosphaeria maculans*. *Fungal Genet. Biol.* **39**: 31–37.
- Idnurm, A., Taylor, J.L., Pedras, M.S.C., and Howlett, B.J.** (2003). Small scale functional genomics of the blackleg fungus, *Leptosphaeria maculans*: Analysis of a 38 kb region. *Australas. Plant Pathol.* **32**: 511–519.
- Jaffe, D.B., Butler, J., Gnerre, S., Maucelli, E., Lindblad-Toh, K., Mesirov, J.P., Zody, M.C., and Lander, E.S.** (2003). Whole genome sequence assembly for mammalian genomes: Arachne 2. *Genome Res.* **13**: 91–96.
- James, T., et al.** (2006). Reconstructing the early evolution of fungi using a six-gene phylogeny. *Nature* **443**: 818–822.
- Jones, T., Federspiel, N.A., Chibana, H., Dungan, J., Kalman, S., Magee, B.B., Newport, G., Thorstenson, Y.R., Agabian, N., Magee, P.T., Davis, R.W., and Scherer, S.** (2004). The diploid genome sequence of *Candida albicans*. *Proc. Natl. Acad. Sci. USA* **101**: 7329–7334.
- Kall, L., Krogh, A., and Sonnhammer, E.L.** (2004). A combined transmembrane topology and signal peptide prediction method. *J. Mol. Biol.* **338**: 1027–1036.
- Kamper, J., et al.** (2006). Insights from the genome of the biotrophic fungal plant pathogen *Ustilago maydis*. *Nature* **444**: 97–101.
- Keon, J., Antoniw, J., Rudd, J., Skinner, W., Hargreaves, J., and Hammond-Kosack, K.** (2005). Analysis of expressed sequence tags from the wheat leaf blotch pathogen *Mycosphaerella graminicola* (anamorph *Septoria tritici*). *Fungal Genet. Biol.* **42**: 376–389.
- Kim, K.-H., Cho, Y., La Rota, M., Cramer, R.A., Jr., and Lawrence, C.B.** (2007). Functional analysis of the *Alternaria brassicicola* non-ribosomal peptide synthetase gene AbNPS2 reveals a role in conidial cell wall construction. *Mol. Plant Pathol.* **8**: 23–29.
- Kodsueb, R., Dhanasekaran, V., Aptroot, A., Lumyong, P., McKenzie, E.H.C., Hyde, K.D., and Jeewon, R.** (2006). The family Pleosporaceae: Intergeneric relationships and phylogenetic perspectives based on sequence analyses of partial 28S rDNA. *Mycologia* **98**: 571–583.
- Kouvelis, V., Ghikas, D., and Typas, M.** (2004). The analysis of the complete mitochondrial genome of *Lecanicillium muscarium* (synonym *Verticillium lecanii*) suggests a minimum common gene organization in mtDNAs of Sordariomycetes: Phylogenetic implications. *Fungal Genet. Biol.* **41**: 930–940.
- Krogh, A., Larsson, B., von Heijne, G., and Sonnhammer, E.L.** (2001). Predicting transmembrane protein topology with a hidden Markov model: Application to complete genomes. *J. Mol. Biol.* **305**: 567–580.
- Kroken, S., Glass, N.L., Taylor, J.W., Yoder, O.C., and Turgeon, B.G.** (2003). Phylogenomic analysis of type I polyketide synthase genes in pathogenic and saprobic ascomycetes. *Proc. Natl. Acad. Sci. USA* **100**: 15670–15675.
- Kulkarni, R.D., Kelkar, H.S., and Dean, R.A.** (2003). An eight-cysteine-containing CFEM domain unique to a group of fungal membrane proteins. *Trends Biochem. Sci.* **28**: 118–121.
- Lafon, A., Han, K.H., Seo, J.A., Yu, J.H., and d'Enfert, C.** (2006). G-protein and cAMP-mediated signaling in aspergilli: A genomic perspective. *Fungal Genet. Biol.* **43**: 490–502.
- Lee, B.N., Kroken, S., Chou, D.Y.T., Robbertse, B., Yoder, O.C., and Turgeon, B.G.** (2005). Functional analysis of all nonribosomal peptide synthetases in *Cochliobolus heterostrophus* reveals a factor, NPS6, involved in virulence and resistance to oxidative stress. *Eukaryot. Cell* **4**: 545–555.
- Lewis, S.E., et al.** (2002). Apollo: A sequence annotation editor. *Genome Biol.* **3**: 82.
- Linder, M.B., Szilvay, G.R., Nakari-Setälä, T., and Penttilä, M.E.** (2005). Hydrophobins: The protein-amphiphiles of filamentous fungi. *FEMS Microbiol. Rev.* **29**: 877–896.
- Liu, Z., Friesen, T., Ling, H., Meinhardt, S., Oliver, R., Rasmussen, J., and Faris, J.** (2006). The Tsn1-ToxA interaction in the wheat-*Stagonospora nodorum* pathosystem parallels that of the wheat-tan spot system. *Genome* **49**: 1265–1273.
- Liu, Z.H., Faris, J.D., Meinhardt, S.W., Ali, S., Rasmussen, J.B., and Friesen, T.L.** (2004a). Genetic and physical mapping of a gene conditioning sensitivity in wheat to a partially purified host-selective toxin produced by *Stagonospora nodorum*. *Phytopathology* **94**: 1056–1060.
- Liu, Z.H., Friesen, T.L., Rasmussen, J.B., Ali, S., Meinhardt, S.W., and Faris, J.D.** (2004b). Quantitative trait loci analysis and mapping of seedling resistance to *Stagonospora nodorum* leaf blotch in wheat. *Phytopathology* **94**: 1061–1067.
- Lowe, T.M., and Eddy, S.R.** (1997). tRNAscan-SE: A program for improved detection of transfer RNA genes in genomic sequences. *Nucleic Acids Res.* **25**: 955–964.
- Majoros, W.H., Pertea, M., Antonescu, C., and Salzberg, S.L.** (2003). GlimmerM, Exonomy and Unveil: Three ab initio eukaryotic gene-finders. *Nucleic Acids Res.* **31**: 3601–3604.
- Manning, V.A., Andrie, R.M., Trippe, A.F., and Ciuffetti, L.M.** (2004). Ptr ToxA requires multiple motifs for complete activity. *Mol. Plant Microbe Interact.* **17**: 491–501.
- Manning, V.A., and Ciuffetti, L.M.** (2005). Localization of Ptr ToxA produced by *Pyrenophora tritici-repentis* reveals protein import into wheat mesophyll cells. *Plant Cell* **17**: 3203–3212.
- Marchler-Bauer, A., et al.** (2005). CDD: A Conserved Domain Database for protein classification. *Nucleic Acids Res.* **33**: D192–D196.
- Marchler-Bauer, A., and Bryant, S.H.** (2004). CD-Search: Protein domain annotations on the fly. *Nucleic Acids Res.* **32**: W327–331.
- Meinhardt, S.W., Cheng, W.J., Kwon, C.Y., Donohue, C.M., and Rasmussen, J.B.** (2002). Role of the arginyl-glycyl-aspartic motif in the action of Ptr ToxA produced by *Pyrenophora tritici-repentis*. *Plant Physiol.* **130**: 1545–1551.
- Moriwaki, A., Kihara, J., Kobayashi, T., Tokunaga, T., Arase, S., and Honda, Y.** (2004). Insertional mutagenesis and characterization of a polyketide synthase gene (PKS1) required for melanin biosynthesis in *Bipolaris oryzae*. *FEMS Microbiol. Lett.* **238**: 1–8.

- Needleman, S.B., and Wunsch, C.D.** (1970). A general method applicable to the search for similarities in the amino acid sequence of two proteins. *J. Mol. Biol.* **48**: 443–453.
- Nicholson, T.P., Rudd, B.A., Dawson, M., Lazarus, C.M., Simpson, T.J., and Cox, R.J.** (2001). Design and utility of oligonucleotide gene probes for fungal polyketide synthases. *Chem. Biol.* **8**: 157–178.
- Oide, S., Moeder, W., Krasnoff, S., Gibson, D., Haas, H., Yoshioka, K., and Turgeon, B.G.** (2006). NPS6, encoding a nonribosomal peptide synthetase involved in siderophore-mediated iron metabolism, is a conserved virulence determinant of plant pathogenic ascomycetes. *Plant Cell* **18**: 2836–2853.
- Oliver, R.P., and Ipcho, S.V.S.** (2004). Arabidopsis pathology breathes new life into the necrotrophs vs. biotrophs classification of fungal pathogens. *Mol. Plant Pathol.* **5**: 347–352.
- Orbach, M.** (1989). Electrophoretic characterisation of the *Magnaporthe grisea* genome. *Fungal Genet. Newsl.* **14**: 14.
- Orbach, M., Vollrath, D., Davis, R., and Yanofsky, C.** (1988). An electrophoretic karyotype for *Neurospora crassa*. *Mol. Cell. Biol.* **8**: 1469–1473.
- Padovan, A.C., Sanson, G.F., Brunstein, A., and Briones, M.R.** (2005). Fungi evolution revisited: Application of the penalized likelihood method to a bayesian fungal phylogeny provides a new perspective on phylogenetic relationships and divergence dates of ascomycota groups. *J. Mol. Evol.* **60**: 726–735.
- Peng, T., Shubitz, L., Simons, J., Perrill, R., Orsborn, K.I., and Galgiani, J.N.** (2002). Localization within a proline-rich antigen (Ag2/PRA) of protective antigenicity against infection with *Coccidioides immitis* in mice. *Infect. Immun.* **70**: 3330–3335.
- Price, A.L., Jones, N.C., and Pevzner, P.A.** (2005). De novo identification of repeat families in large genomes. *Bioinformatics* **21**(Suppl 1): i351–i358.
- Proctor, R.H., Desjardins, A.E., Plattner, R.D., and Hohn, T.M.** (1999). A polyketide synthase gene required for biosynthesis of fumonisin mycotoxins in *Gibberella fujikuroi* mating population A. *Fungal Genet. Biol.* **27**: 100–112.
- Rawson, J.M.** (2000). Transposable Elements in the Phytopathogenic Fungus *Stagonospora nodorum*. PhD dissertation (Birmingham, UK: University of Birmingham).
- Rice, P., Longden, I., and Bleasby, A.** (2000). EMBOSS: The European Molecular Biology Open Software Suite. *Trends Genet.* **16**: 276–277.
- Richards, T.A., Dacks, J.B., Jenkinson, J.M., Thornton, C.R., and Talbot, N.J.** (2006). Evolution of filamentous plant pathogens: Gene exchange across eukaryotic kingdoms. *Curr. Biol.* **16**: 1857–1864.
- Robbertse, B., Reeves, J.B., Schoch, C.L., and Spatafora, J.W.** (2006). A phylogenomic analysis of the Ascomycota. *Fungal Genet. Biol.* **43**: 715–725.
- Rodriguez, F., Oliver, J.F., Martin, A., and Medina, J.R.** (1990). The general stochastic model of nucleotide substitution. *J. Theor. Biol.* **142**: 485–501.
- Schoch, C.L., Shoemaker, R.A., Seifert, K.A., Hambleton, S., Spatafora, J.W., and Crous, P.W.** (2006). A multigene phylogeny of the Dothideomycetes using four nuclear loci. *Mycologia* **98**: 1041–1052.
- Shimizu, T., Kinoshita, H., Ishihara, S., Sakai, K., Nagai, S., and Nihira, T.** (2005). Polyketide synthase gene responsible for citrinin biosynthesis in *Monascus purpureus*. *Appl. Environ. Microbiol.* **71**: 3453–3457.
- Solomon, P.S., Tan, K.-C., and Oliver, R.P.** (2003a). The nutrient supply of pathogenic fungi; a fertile field for study. *Mol. Plant Pathol.* **4**: 203–210.
- Solomon, P.S., Thomas, S.W., Spanu, P., and Oliver, R.P.** (2003b). The utilisation of di/tripeptides by *Stagonospora nodorum* is dispensable for wheat infection. *Physiol. Mol. Plant Pathol.* **63**: 191–199.
- Solomon, P.S., Lee, R.C., Wilson, T.J.G., and Oliver, R.P.** (2004a). Pathogenicity of *Stagonospora nodorum* requires malate synthase. *Mol. Microbiol.* **53**: 1065–1073.
- Solomon, P.S., Lowe, R.G.T., Tan, K.-C., Waters, O.D.C., and Oliver, R.P.** (2006a). *Stagonospora nodorum*: cause of stagonospora nodorum blotch of wheat. *Mol. Plant Pathol.* **7**: 147–156.
- Solomon, P.S., Tan, K.C., Sanchez, P., Cooper, R.M., and Oliver, R.P.** (2004b). The disruption of a G alpha subunit sheds new light on the pathogenicity of *Stagonospora nodorum* on wheat. *Mol. Plant Microbe Interact.* **17**: 456–466.
- Solomon, P.S., Waters, O.D., Simmonds, J., Cooper, R.M., and Oliver, R.P.** (2005). The Mak2 MAP kinase signal transduction pathway is required for pathogenicity in *Stagonospora nodorum*. *Curr. Genet.* **48**: 60–68.
- Solomon, P.S., Wilson, T.J.G., Rybak, K., Parker, K., Lowe, R.G.T., and Oliver, R.P.** (2006b). Structural characterisation of the interaction between *Triticum aestivum* and the dothideomycete pathogen *Stagonospora nodorum*. *Eur. J. Plant Pathol.* **114**: 275–282.
- Spatafora, J.W., et al.** (2006). A five-gene phylogenetic analysis of the Pezizomycotina. *Mycologia* **98**: 1018–1028.
- Stamatakis, A.** (2006). RAxML-VI-HPC: Maximum likelihood-based phylogenetic analyses with thousands of taxa and mixed models. *Bioinformatics* **22**: 2688–2690.
- Stukenbrock, E.H., Banke, S., and McDonald, B.A.** (2006). Global migration patterns in the fungal wheat pathogen *Phaeosphaeria nodorum*. *Mol. Ecol.* **15**: 2895–2904.
- Stukenbrock, E.H., and McDonald, B.A.** (2007). Geographic variation and positive diversifying selection in the host specific toxin *SnToxA*. *Mol. Plant Pathol.* **8**: 321–322.
- Sumii, M., Furutani, Y., Waschuk, S.A., Brown, L.S., and Kandori, H.** (2005). Strongly hydrogen-bonded water molecule present near the retinal chromophore of *Leptosphaeria rhodopsin*, the bacteriorhodopsin-like proton pump from a eukaryote. *Biochemistry* **44**: 15159–15166.
- Talbot, N., Salch, Y., Ma, M., and Hamer, J.** (1993). Karyotypic variation within clonal lineages of the rice blast fungus, *Magnaporthe grisea*. *Appl. Environ. Microbiol.* **59**: 585–593.
- Talbot, N.J., McCafferty, H.R.K., Ma, M., Moore, K., and Hamer, J.E.** (1997). Nitrogen starvation of the rice blast fungus *Magnaporthe grisea* may act as an environmental cue for disease symptom expression. *Physiol. Mol. Plant Pathol.* **50**: 179–195.
- Tambor, J., Guedes, R., Nobrega, M., and Nobrega, F.** (2006). The complete DNA sequence of the mitochondrial genome of the dermatophyte fungus *Epidermophyton floccosum*. *Curr. Genet.* **49**: 302–308.
- Thomma, B., Bolton, M.D., Clergeot, P.H., and De Wit, P.** (2006). Nitrogen controls in planta expression of *Cladosporium fulvum* Avr9 but no other effector genes. *Mol. Plant Pathol.* **7**: 125–130.
- Thompson, J.D., Gibson, T.J., Plewniak, F., Jeanmougin, F., and Higgins, D.G.** (1997). The CLUSTAL_X windows interface: Flexible strategies for multiple sequence alignment aided by quality analysis tools. *Nucleic Acids Res.* **25**: 4876–4882.
- Trail, F., Xu, J.R., San Miguel, P., Halgren, R.G., and Kistler, H.C.** (2003). Analysis of expressed sequence tags from *Gibberella zeae* (anamorph *Fusarium graminearum*). *Fungal Genet. Biol.* **38**: 187–197.
- Vizzaino, J.A., Cardoza, R.E., Dubost, L., Bodo, B., Gutierrez, S., and Monte, E.** (2006). Detection of peptaibols and partial cloning of a putative peptaibol synthetase gene from *T. harzianum* CECT 2413. *Folia Microbiol. (Praha)* **51**: 114–120.
- Wessels, J.G.H.** (1994). Developmental regulation of fungal cell wall formation. *Annu. Rev. Phytopathol.* **32**: 413–437.
- Winefield, R.D., Hilario, E., Beever, R.E., Haverkamp, R.G., and Templeton, M.D.** (2007). Hydrophobin genes and their expression in conidial and aconidial *Neurospora* species. *Fungal Genet. Biol.* **44**: 250–257.

- Winka, K., and Eriksson, O.E.** (1997). Supraordinal taxa of Ascomycota. *Mol Phylogenet Evol.* **1**: 1–16.
- Wolpert, T.J., Dunkle, L.D., and Ciuffetti, L.M.** (2002). Host-selective toxins and avirulence determinants: What's in a name? *Annu. Rev. Phytopathol.* **40**: 251–285.
- Woo, P., et al.** (2003). The mitochondrial genome of the thermal dimorphic fungus *Penicillium marneffei* is more closely related to those of molds than yeasts. *FEBS Lett.* **555**: 469–477.
- Yadav, G., Gokhale, R.S., and Mohanty, D.** (2003). SEARCHPKS: A program for detection and analysis of polyketide synthase domains. *Nucleic Acids Res.* **31**: 3654–3658.
- Yoder, O.C., and Turgeon, B.G.** (2001). Fungal genomics and pathogenicity. *Curr. Opin. Plant Biol.* **4**: 315–321.
- Yun, S.H., Turgeon, B.G., and Yoder, O.C.** (1998). REMI-induced mutants of *Mycosphaerella zeae-maydis* lacking the polyketide PM-toxin are deficient in pathogenesis to corn. *Physiol. Mol. Plant Pathol.* **52**: 53–66.
- Zhang, Z., Schwartz, S., Wagner, L., and Miller, W.** (2000). A greedy algorithm for aligning DNA sequences. *J. Comput. Biol.* **7**: 203–214.
- Zolan, M.E.** (1995). Chromosome-length polymorphism in fungi. *Microbiol. Rev.* **59**: 686–698.

Dothideomycete Plant Interactions Illuminated by Genome Sequencing and EST Analysis of the Wheat Pathogen *Stagonospora nodorum*

James K. Hane, Rohan G.T. Lowe, Peter S. Solomon, Kar-Chun Tan, Conrad L. Schoch, Joseph W. Spatafora, Pedro W. Crous, Chinappa Kodira, Bruce W. Birren, James E. Galagan, Stefano F.F. Torriani, Bruce A. McDonald and Richard P. Oliver
PLANT CELL 2007;19;3347-3368; originally published online Nov 16, 2007;
DOI: 10.1105/tpc.107.052829

This information is current as of February 18, 2010

Supplemental Data	http://www.plantcell.org/cgi/content/full/tpc.107.052829/DC1
References	This article cites 124 articles, 44 of which you can access for free at: http://www.plantcell.org/cgi/content/full/19/11/3347#BIBL
Permissions	https://www.copyright.com/ccc/openurl.do?sid=pd_hw1532298X&issn=1532298X&WT.mc_id=pd_hw1532298X
eTOCs	Sign up for eTOCs for <i>THE PLANT CELL</i> at: http://www.plantcell.org/subscriptions/etoc.shtml
CiteTrack Alerts	Sign up for CiteTrack Alerts for <i>Plant Cell</i> at: http://www.plantcell.org/cgi/alerts/ctmain
Subscription Information	Subscription information for <i>The Plant Cell</i> and <i>Plant Physiology</i> is available at: http://www.aspb.org/publications/subscriptions.cfm